

Should we care about the level of detail in trees when running urban microscale simulations?

Fu, Runnan; Pađen, Ivan; García-Sánchez, Clara

DOI

[10.1016/j.scs.2023.105143](https://doi.org/10.1016/j.scs.2023.105143)

Publication date

2024

Document Version

Final published version

Published in

Sustainable Cities and Society

Citation (APA)

Fu, R., Pađen, I., & García-Sánchez, C. (2024). Should we care about the level of detail in trees when running urban microscale simulations? *Sustainable Cities and Society*, 101, Article 105143. <https://doi.org/10.1016/j.scs.2023.105143>

Important note

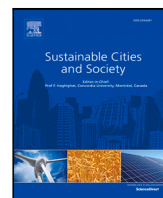
To cite this publication, please use the final published version (if applicable). Please check the document version above.

Copyright

Other than for strictly personal use, it is not permitted to download, forward or distribute the text or part of it, without the consent of the author(s) and/or copyright holder(s), unless the work is under an open content license such as Creative Commons.

Takedown policy

Please contact us and provide details if you believe this document breaches copyrights. We will remove access to the work immediately and investigate your claim.



Should we care about the level of detail in trees when running urban microscale simulations?

Runnan Fu^{*}, Ivan Pađen, Clara García-Sánchez

3D Geoinformation Research Group, Delft University of Technology, Delft, Netherlands

ARTICLE INFO

Dataset link: https://github.com/furunnan/Tre_e_Topo_Effects_on_Wind

Keywords:

CFD
Wind flow
Tree model
Level of detail
Urban area

ABSTRACT

Due to lack of information and long geometry generation times, tree geometries are usually oversimplified or even ignored in Computational Fluid Dynamic (CFD) simulations that predict wind and pollutant dispersion in urban areas. Nevertheless, trees are known to impact local wind patterns and air quality levels. Thus, in this paper we explore the effects that tree models automatically reconstructed at diverse Level of Detail (LoD) (1, 2 and 3) have in numerical wind predictions. We address this by comparing the non-dimensional velocity magnitude differences between simulations with multiple tree LoDs. To further understand these differences in changing environmental contexts we use three morphologies: an isolated tree, an idealized street, canyon, and a real urban geometry from Rotterdam, The Netherlands. The numerical results show that the velocity magnitude differences between the cases with LoD1 tree models and those with LoD2 tree models can be over 1.0 m/s while the differences between LoD2 and LoD3 cases are rather limited, usually lower than 0.2 m/s. Consequently, through this study we highlight the importance of using tree models in LoD2 or LoD3 at least for CFD simulations of wind flows in urban areas. To further support this conclusion we also analyze the impact of changing wind directions and tree Leaf Area Density (LAD) values in the impact of tree LoDs on wind. The differences found in this work linked to the level of realism in your tree models can support future studies where researchers want to make an informed choice.

1. Introduction

With more and more people living in urban areas, urbanization is expanding. As a result of this increase in urbanization comes a rise of human activities which is linked to problems such as the rising temperatures (Urban Heat Islands (UHI), especially at night) and air pollution in cities, which eventually can lead to various diseases and premature deaths (Fouillet et al., 2006; Salmond et al., 2016). Since a good urban wind environment can ameliorate air quality, mitigate heat island effects, improve pedestrian wind comfort and reduce buildings energy consumption, this field of research is currently receiving enhanced attention (Blocken et al., 2012; Hsieh & Huang, 2016).

A widely considered economical and effective way to create a good urban wind environment is the planting of trees (Aflaki et al., 2017; Salmond et al., 2016; Szkordilis & Zöld, 2016), as trees can affect the wind flow by reducing its speed and changing its direction (Szkordilis & Zöld, 2016). Yet, trees may also have a negative impact on local air quality even if they promote deposition of pollutants in their leaves, because they reduce ventilation (Buccolieri et al., 2018). It is worth noting that the dynamic effects of trees on the urban wind environment depends not only on environmental factors such as the surrounding

built environment, local climate and wind speed, but also on tree properties such as tree shape, height and foliage density which may also be linked to seasonality (Hefny Salim et al., 2015; Manickathan et al., 2018). In order to assess tree effects and find suitable tree layouts in diverse urban areas, Computational Fluid Dynamics (CFD) simulations can be used.

There has been a lot of interest in using CFD models to study tree effects. Current studies have focused on the effects on air quality (Balczó et al., 2009; Moradpour et al., 2017; Santiago et al., 2019; Vos et al., 2013), pedestrian wind comfort (Hong & Lin, 2015; Kang et al., 2020; Ricci et al., 2022) and the thermal urban environment (Gromke et al., 2015; Hong & Lin, 2015; Manickathan et al., 2018). However, despite the fact that the importance of trees has been demonstrated in many studies, for practical purposes and/or lack of information, the geometric features of trees are usually oversimplified or even ignored in CFD wind simulations over urban areas (Hefny Salim et al., 2015). A relevant example was already published by Manickathan (2019), where the author found that CFD predictions tend to underestimate the wake velocity deficit compared to experimental measurements due to oversimplification of the tree geometry.

^{*} Correspondence to: Faculty of Architecture and the Built Environment, Julianalaan 134, 2628 BL, Delft, Netherlands.

E-mail addresses: runnan_fu@outlook.com (R. Fu), i.paden@tudelft.nl (I. Pađen), c.garcia-sanchez@tudelft.nl (C. García-Sánchez).

Just as buildings, trees can be expressed in different levels of abstractions, also known as levels of detail (LoDs). For buildings, typically the classification by Biljecki et al. (2016) is used. However, when it comes to tree reconstruction, there are still no standardized nor widely adopted classifications. A number of other authors proposed their own classifications, such as Chen (2013), Liang et al. (2016) and Ortega-Córdova (2018). de Groot (2020) proposed a classification for their automatic reconstruction workflow, guided by the input data which was the airborne LiDAR. Since this classification can be very efficiently applied in the context of urban wind flow studies, we will be using it throughout the paper. The classification is introduced in Section 2.1. And while the effect of building LoDs on wind flow has been examined in the past (García-Sánchez et al., 2021; Ricci et al., 2017), this kind of exploratory investigation for trees has yet to be conducted, to the best of our knowledge.

Although several studies have been conducted in the past that feature tree models with varying levels of realism, there is little consensus on how to systematically include trees in urban flow simulations. This is extremely important when limited data on the tree structure is available. To the best of our knowledge, our approach is the first to benefit from automatic tree reconstruction at multiple levels of detail to amend this lack of data, which is a common issue in urban flow simulations. With this approach we aim to address the question: what is the impact of different LoDs and tree shapes on the wind flow structure? For that, we use systematic tree model definitions in LoD1, LoD2 and LoD3 in numerical simulations with different urban complexities. The comparative analysis also includes several leaf area density (LAD) values and wind directions.

Before carrying out our work, we validated our CFD model with the tree drag terms introduced in Section 2.2 using the tree model and setup from Manickathan (2019). Despite being subject to a certain level of uncertainty, by comparing a number of test cases, we are able to summarize the trend of tree LoD effects on wind. This allows us to highlight the impact of tree LoD in CFD simulations of wind flows in urban areas of different complexities. By understanding how important wind speed changes are depending on the level of detail, we may guide decisions for future urban flow simulations, minimizing resources usage while maximizing predictability.

2. Materials and methods

2.1. Tree LoDs and their automatic reconstruction

The tree LoD classification we are using was originally proposed by de Groot (2020). The classification is relying on abstraction levels attainable from an airborne LiDAR-based automatic reconstruction algorithm. The obtained LoD1 model is cylindrical or prismatic, with only a canopy. Trees in LoD2 are implicit volumetric models, based on pre-made models and scaled in width and height. LoD3 are parametric models based on parameters extracted from a collection of points representing a tree. These levels of abstractions, or at least canopy shapes similar to those LoDs, are typically observed in numerical investigations, e.g. Amorim et al. (2013), Hefny Salim et al. (2015), Kang et al. (2020), Kenjereš and Ter Kuile (2013), Santiago et al. (2019), Sousa and Gorlé (2019) for LoD1, Hong et al. (2018a, 2018b) for LoD2, and Brozovsky et al. (2022, 2021) for LoD3.

Overall, seven types of tree models are used in this work (a-g) (included in Fig. 1), namely LoD1 tree, LoD2 broadleaf, LoD3 broadleaf, LoD2 conifer, and LoD3 conifer model. LoD1 tree (a), LoD2 broadleaf (c), LoD3 broadleaf (d), LoD2 conifer (f), and LoD3 conifer (g) are generated using the automatic tree reconstruction algorithm proposed by de Groot (2020). LoD1 is defined as a model that does not take into account the specific shape of the tree crown and represents it with the simplest rectangle. This model is also used in some practical applications and past research (Mohamed & Wood, 2015). However, it should be noted that other studies take into account the influence

of the tree stem and remove the tree stem portion from the LoD1 model (Jeanjean et al., 2015; Maison et al., 2022). In order to provide effective recommendations for this area of research, we have also added two LoD1 models without tree stems (b, e) for the simulations.

2.2. Tree porosity model

To handle trees in CFD simulations, finite volume cells that roughly account for tree canopies are marked as porous zones while tree stems are modeled explicitly as obstacles, as done in Hefny Salim et al. (2015), Kang et al. (2020) and Manickathan (2019). In these porous zones, tree drag is represented by adding a sink term (S_{u_i}) in the momentum equation and source terms (S_k and S_ϵ) in the turbulence equations (Katul et al., 2004; Kenjereš & Ter Kuile, 2013; Sanz, 2003).

$$S_{u_i} = -\rho C_d LAD U_i |U| \left[\frac{N}{m^3} \right] \quad (1)$$

$$S_k = \rho C_d LAD (\beta_p |U|^3 - \beta_d |U|k) \left[\frac{W}{m^3} \right] \quad (2)$$

$$S_\epsilon = \rho C_d LAD \frac{\epsilon}{k} (C_{\epsilon 4} \beta_p |U|^3 - C_{\epsilon 5} \beta_d |U|k) \left[\frac{W}{m^3 s} \right] \quad (3)$$

Eq. (1) is the sink term for the momentum equation, Eq. (2) is the source term for the turbulence kinetic energy equation, and Eq. (3) is the source term for the turbulent dissipation rate equation; ρ is the air density, C_d is the leaf drag coefficient, LAD is the leaf area density, U_i is the velocity component in direction i , $|U|$ is the wind speed magnitude, β_p is the fraction of mean kinetic energy converted into turbulent kinetic energy, β_d is the dimensionless coefficient for the short-circuiting of turbulent cascade, $C_{\epsilon 4}$ and $C_{\epsilon 5}$ are model constants. Depending on the studied cases, several values for β_p , β_d , $C_{\epsilon 4}$ and $C_{\epsilon 5}$ could be found in literature (Buccolieri et al., 2018; Hefny Salim et al., 2015; Hong et al., 2018a; Liang et al., 2006; Santiago et al., 2019). Usually, β_p is assumed equal to 1 and the values for β_d , $C_{\epsilon 4}$ and $C_{\epsilon 5}$ range between 4–6.5, 0.9–2 and 0.9–1.8, respectively (Buccolieri et al., 2018).

In this paper, the value of the drag coefficient C_d is defined as a constant (0.2), which is consistent with most of the literature (Gromke et al., 2015). The values of β_p , β_d , $C_{\epsilon 4}$ and $C_{\epsilon 5}$ are set to 1, 5.1, 0.9 and 0.9 (Buccolieri et al., 2018), respectively.

LAD, defined as the one-side leaf surface area per unit volume ($m^2 m^{-3}$), depends on tree species and varies with height over the tree crown. The values used in CFD simulations range from 0.1 to 4, with an average value in the literature about 1 (Buccolieri et al., 2018). In this paper, the value of LAD is assumed to be spatially constant. The reason is that this paper focuses on comparing the effects of different tree LoDs without scrutinizing the LAD profile of an individual tree. Also, both varying LAD distribution and the constant (spatially-averaged) LAD value have been shown to behave similarly in CFD predictions (Manickathan, 2019).

2.3. Test cases design and set up

In order to analyze the impact of tree LoD in wind patterns broadly, we selected urban environments with diverse complexity. We considered three morphologies: an isolated tree, an idealized street canyon, and a real urban geometry (corresponding to a region of Rotterdam, The Netherlands). For tree types, broadleaf and conifer trees are considered.

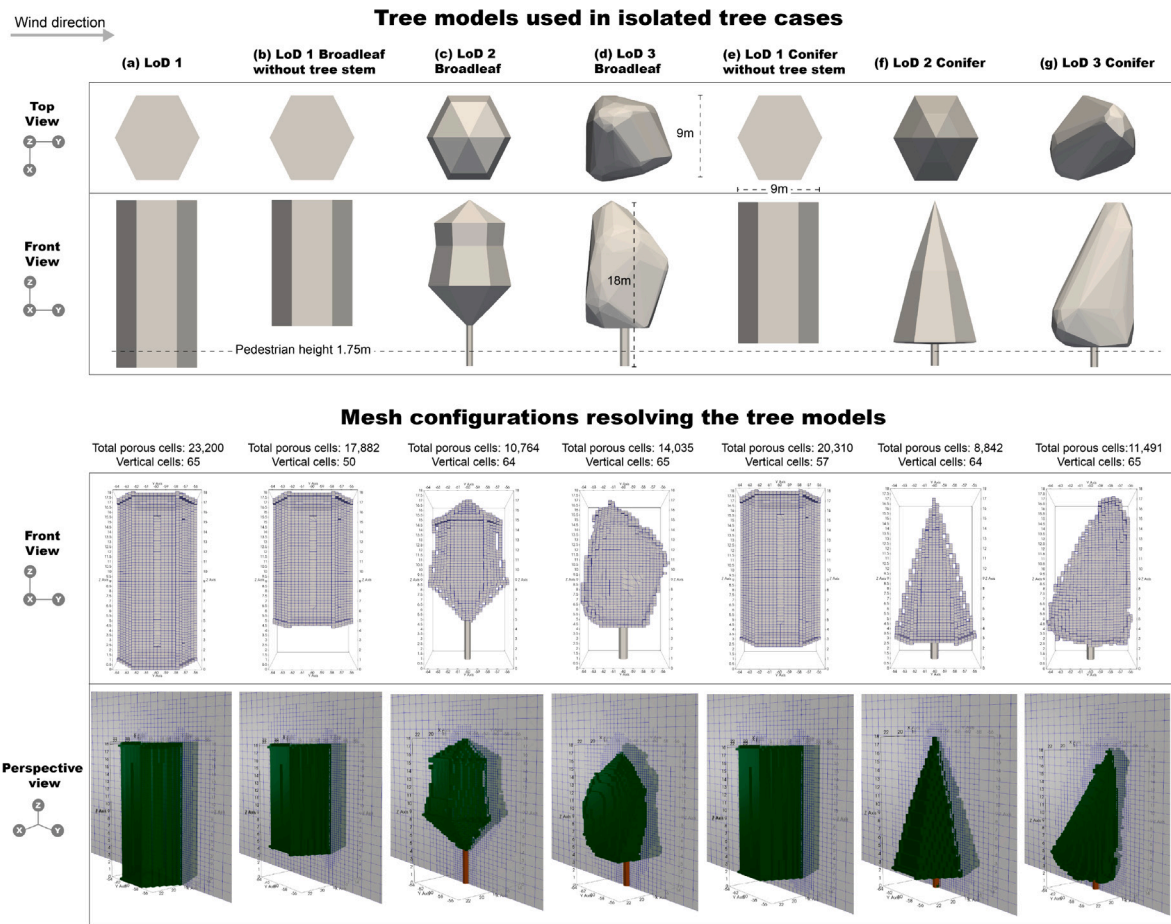


Fig. 1. The tree models and the mesh configurations used in isolated tree cases. Models (a), (c), (d), (f), (g) are generated using the tree LoD classification proposed by de Groot (2020). To study the effect of tree stem, we also use models (b) and (e) for the simulations. Tree stem is explicitly modeled as an obstacle while canopy is modeled as porous cells. Vertical cells refers to the number of layers across the tree models. Total porous cells refers to the number of cells resolving the tree canopy.

2.3.1. Isolated tree

As Fig. 1 shows, seven types of tree models are used in isolated tree cases.

These tree models have a uniform bounding box size, i.e., 8 m in length and width and 18 m in height. The stem portion of the LoD2 and LoD3 trees is explicitly modeled as an obstacle that does not allow wind to pass through, which is consistent with the reality. The LoD1 tree, however, have only a canopy, which is implicitly modeled as a porous area that allows wind to pass through.

For each test case, the same meteorological conditions are used: the wind blows in the Y-axis with an inflow velocity of 4.97 m s^{-1} at 10 m above the ground, and this is consistent with local measurements in Rotterdam already used to study the impact of building LoD on CFD predictions García-Sánchez et al. (2021). The flow is considered incompressible and the atmospheric boundary layer (ABL) stratification is assumed to be neutral.

2.3.2. Idealized street canyon

Inspired by the street canyon and avenue-like tree configurations of Gromke et al. (2012) and CODASC (Concentration Data of Street Canyons),¹ we make the street canyon representation of each case consists of two parallel-aligned building blocks (length $L = 180 \text{ m}$, height $H = 18 \text{ m}$, width $W = 18 \text{ m}$, aspect ratio $W/H = 1$) and a row of tree models placed in the middle with a gap of 15 m. The same

tree models in the isolated tree cases (Fig. 1) are used in the street canyon test cases. Also, two wind directions are used: perpendicular and parallel to buildings, both with the same meteorological conditions as the isolated tree cases.

The wind directions, building arrangements, and tree configuration are shown in Fig. 2.

2.3.3. Realistic urban geometry

Test cases for the realistic urban geometry are mainly used to simulate tree effects on more complex airflow distributions. Complicated street and tree configurations and variations in building shapes result in more complicated flow fields, which allow the effects of tree LoDs and shapes to potentially no longer be confined to local areas. The insights obtained may be important for larger-scale studies of urban wind environments.

The study area is Noordereiland in Rotterdam, which is an island with an area of about 67 hectares. The inflow wind direction for the study area is South-Southwest (SSW) and the inflow wind speed is around 3.7 m/s at 2 m height above the terrain, which are estimated by averaging the wind speed and wind direction data from 2021 provided by the RainGain² project of TU Delft.

With the wind direction of SSW, the bottom boundary of the CFD computational domain can be assumed to be water surface, except for the study area. The building models are obtained through the 3D BAG database Peters et al. (2022), where they are downloaded

¹ CODASC: <https://www.umweltaerodynamik.de/bilder-originale/CODA/CODASC.html>

² RainGain: <https://weather.tudelft.nl/>

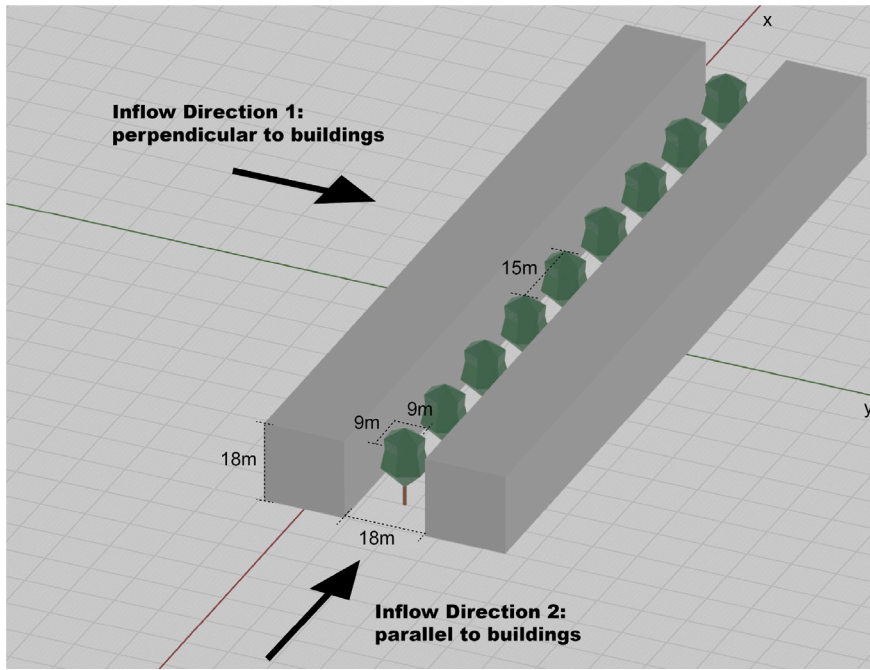


Fig. 2. Wind directions, buildings arrangements and tree configurations of the street canyon cases.

Realistic urban geometry models

Study area: Noordereiland, Rotterdam, the Netherlands

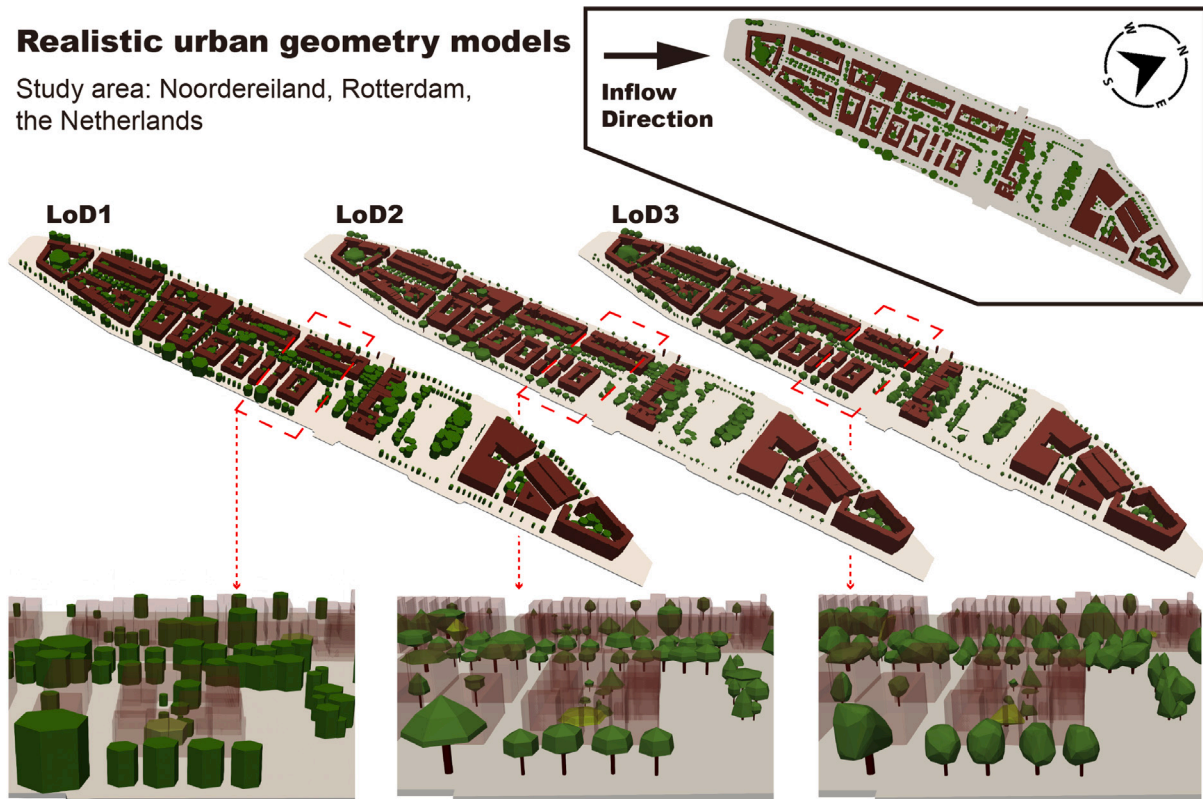


Fig. 3. Different LoD tree configurations for the realistic urban geometry model from Noordereiland in Rotterdam, The Netherlands.

directly as a 3D city model. Trees in the domain are automatically reconstructed using the algorithm adapted from de Groot (2020), based on point clouds obtained using the AHN3 (Actueel Hoogtebestand Nederland PDOK (2021)) point cloud dataset. For the terrain, in order to reduce complexity, we assumed to have a flat ground surface with 2 m height above the water surface. Fig. 3 shows the final models used in the test cases.

2.4. Numerical simulations set up

To perform the CFD simulations, OpenFOAM (version 7) (Weller et al., 1998), an open-source computational fluid dynamics software, is used. We consider the flow incompressible, steady, with neutral stratification, and accordingly we used the Reynolds-Averaged Navier–Stokes (RANS) method to model the flow structures. We acknowledge that

Table 1

Mesh specifications and computational time specified for each case. Vertical cells refers to the number of layers across the tree. ' and '' refer to cases without tree stem.

Case Nr.	Case type	Tree type	Tree stem	LoD	Vertical cells	Total cells	Run time [s]
1	isolated	–	no	1	65	168 192	97
1'	isolated	broadleaf	no	1	50	165 147	102
1''	isolated	conifer	no	1	57	168 325	102
2	isolated	broadleaf	yes	2	64	154 657	88
3	isolated	broadleaf	yes	3	65	159 970	94
4	isolated	conifer	yes	2	64	148 522	83
5	isolated	conifer	yes	3	65	157 058	92
6	canyon	–	no	1	65	932 417	817
6'	canyon	broadleaf	no	1	50	922 582	889
6''	canyon	conifer	no	1	57	932 487	1431
7	canyon	broadleaf	yes	2	64	883 962	1159
8	canyon	broadleaf	yes	3	65	895 589	2444
9	canyon	conifer	yes	2	64	872 840	1112
10	canyon	conifer	yes	3	65	891 166	2549
11	canyon	–	no	1	65	932 417	892
11'	canyon	broadleaf	no	1	50	922 582	1401
11''	canyon	conifer	no	1	57	932 487	956
12	canyon	broadleaf	yes	2	64	883 962	2528
13	canyon	broadleaf	yes	3	65	895 589	2714
14	canyon	conifer	yes	2	64	872 840	2548
15	canyon	conifer	yes	3	65	891 166	2456
16	real	–	no	1	–	7 476 244	8446
17	real	broadleaf & conifer	yes	2	–	6 849 710	22 696
18	real	broadleaf & conifer	yes	3	–	7 116 564	21 241

higher fidelity methods, such as Large Eddy Simulations, are available and have been used in the past for urban flows by other authors (Ma et al., 2022; Salim et al., 2011; Zheng & Yang, 2021). These methods, although proven to be superior in turbulence representation than RANS when compared to wind tunnel measurements, are prohibitively costly in terms of time and computer resources. Consequently, these methods are rarely used in the design phase, which usually requires several models to be evaluated. Our work specifically targets such design phase, where decisions regarding urban landscape are taken.

2.4.1. Governing equations

As the Reynolds-Averaged Navier–Stokes approach is used for the CFD simulations, the mass and momentum mean conservation equations that govern the flow are the following:

$$\frac{\partial \bar{u}_j}{\partial x_j} = 0 \quad (4)$$

$$\bar{u}_j \frac{\partial \bar{u}_i}{\partial x_j} = -\frac{1}{\rho} \frac{\partial \bar{p}}{\partial x_i} + \nu \frac{\partial^2 \bar{u}_j}{\partial x_j \partial x_j} - \frac{\partial \overline{u'_i u'_j}}{\partial x_j} + F_i \quad (5)$$

where \bar{u}_i denotes time-averaged velocity components, ρ is the density, \bar{p} is the mean pressure, ν is the kinematic viscosity and F_i is the source or sink term. F_i is only considered in porous zones that represent trees, and is equal to Eq. (1). In other cases, it is zero. The term $\overline{u'_i u'_j}$ represents the Reynolds stress tensor, which is unknown and needs to be closed with a turbulence model. For our case, we used the two equations standard $k-\epsilon$ turbulence model since it is widely used in outdoor wind simulations (Blocken, 2015; García-Sánchez et al., 2021). In this model, $\overline{u'_i u'_j}$ is computed based on the linear eddy viscosity hypothesis:

$$\overline{u'_i u'_j} = \frac{2}{3} k \delta_{ij} - 2\mu_t S_{ij} \quad (6)$$

where k is the turbulence kinetic energy, S_{ij} the time-averaged shear stress tensor, and μ_t is the turbulence viscosity, which is computed using following equation:

$$\mu_t = C_\mu \frac{k^2}{\epsilon} \quad (7)$$

where C_μ is a model constant equal to 0.09. The equations for the two turbulence variables, namely the turbulence kinetic energy, k , and the

turbulence dissipation rate, ϵ , are as follows:

$$\bar{u}_j \frac{\partial k}{\partial x_j} = \frac{\partial}{\partial x_j} \left[\left(\nu + \frac{\nu_t}{\sigma_k} \right) \frac{\partial k}{\partial x_j} \right] + P_k - \epsilon + S_k \quad (8)$$

$$\bar{u}_j \frac{\partial \epsilon}{\partial x_j} = \frac{\partial}{\partial x_j} \left[\left(\nu + \frac{\nu_t}{\sigma_\epsilon} \right) \frac{\partial \epsilon}{\partial x_j} \right] + C_{\epsilon 1} \frac{\epsilon}{k} P_k - C_{\epsilon 2} \frac{\epsilon^2}{k} + S_\epsilon \quad (9)$$

where P_k is the turbulent production term and σ_k , σ_ϵ , $C_{\epsilon 1}$ and $C_{\epsilon 2}$ are model constants, with values of 1.0, 1.3, 1.44, and 1.92 (Lauder & Spalding, 1974), respectively.

2.4.2. Computational domain and mesh

For all numerical test cases, the computational domain should be chosen large enough to avoid artificial acceleration of the flow due to flow contraction caused by the boundaries of the computational domain (Blocken, 2015). Conforming to the best practice guidelines prescribed by Blocken (2015) and Franke et al. (2011), the inlet, lateral and top boundaries are set at least $5H_{\max}$ away from the group of building and tree models, where H_{\max} is the height of the tallest geometry. A distance of at least $15H_{\max}$ is kept downstream of the group of buildings and tree models to allow for adequate wake development. The maximum height (H_{\max}) for the different morphologies used in our study corresponds to 18 m, 18 m and 33 m for isolated tree, idealized street canyon, and a real urban geometry, respectively. Table 1 introduces the final mesh size, vertical layers and time spent to run until convergence each of the cases considered within the article. All cases were run in parallel using 4 cores on an AMD EPYC 7542 processor.

In the text below, we include the mesh independence results for the real geometry case. To complete the mesh independence study, we completed the following steps:

- Step 1: Designed a relatively coarse mesh to run the initial simulation and ensure that the residuals converge,
- Step 2: Refined the initial mesh at a constant ratio (1.3 is used in this paper) to obtain at least two new meshes: medium mesh, and fine mesh. Ran simulations on these two meshes and ensure that the residuals converge,
- Step 3: Mesh independence can be considered as achieved when the relative difference between the solutions of the fine mesh and the medium mesh is a certain margin smaller than that of the

Table 2
Properties of the meshes with different resolutions.

Mesh	Smallest cell height (m)	Total number of cells
Coarse	0.52	3038617
Medium	0.4	5710610
Fine	0.3	11390599

medium mesh and the coarse mesh (Roache, 1994). This means that a finer mesh does not significantly change the solution anymore and that using the medium mesh for final simulations is sufficient, which allow us to make a compromise in terms of time and computational resources. If not, continue refining the mesh and repeat.

Figs. A.1, A.2 and Table 2 introduce the probes positions and the three generated meshes for a realistic urban geometry test case (Case 17), and the medium mesh is used for our final CFD simulations. We compute the grid sensitivity analysis using the methods from Celik et al. (2008) which results in Grid Convergence Indices (more specifically, GCI_{fine}^{21}) of 5.6% for velocity magnitude and 4.8% for the turbulence kinetic energy from 90 randomly placed points in the region of interest (as shown in Fig. A.2). This highlights that the medium mesh is adequate for subsequent simulations.

2.4.3. Boundary conditions

The inflow boundary condition is modeled as a fully developed neutral atmospheric boundary layer condition with the following equations for velocity, turbulence kinetic energy, and dissipation rate:

$$U = \frac{u_*}{\kappa} \ln \frac{z + z_0}{z_0} \quad (10)$$

$$k = \frac{u_*^2}{\sqrt{C_\mu}} \quad (11)$$

$$\epsilon = \frac{u_*^3}{\kappa(z + z_0)} \quad (12)$$

where u_* denotes the friction velocity, κ is the von Karman constant with a value of 0.41, and z_0 is the aerodynamic roughness length. The z_0 value is varied depending on the surface taken into account. For the terrain surface to represent the presence of small obstacles ignored in our current 3D city models, we set z_0 to 0.2 m, which corresponds to a ‘rough area’ according to the updated Davenport–Wieringa roughness classification (Blocken, 2015). For water surfaces surrounding the realistic urban case, 0.0002 m is used.

To run the simulation, the standard $k - \epsilon$ turbulence model and the *simpleFoam* solver in OpenFOAM are modified to add the sink/source terms (S_{u_i} , S_k and S_ϵ).

2.5. Measures for quantitative analysis

To better compare the velocity magnitude difference between LoD1, LoD2 and LoD3 cases, CFD prediction data of two cases can be subtracted and normalized to obtain the non-dimensional velocity magnitude difference C_{l2-l1} , C_{l2-l1}^* and C_{l2-l3} :

$$C_{l2-l1} = \frac{(|U|_{lod2} - |U|_{lod1})}{|U|_{ref}} \quad (13)$$

$$C_{l2-l1}^* = \frac{(|U|_{lod2} - |U|_{lod1\text{WithoutTreeStem}})}{|U|_{ref}} \quad (14)$$

$$C_{l2-l3} = \frac{(|U|_{lod2} - |U|_{lod3})}{|U|_{ref}} \quad (15)$$

where $|U|_{lod1}$, $|U|_{lod1\text{WithoutTreeStem}}$, $|U|_{lod2}$ and $|U|_{lod3}$ represent the velocity magnitude predictions of a case using LoD1 tree models, a case using LoD1 without tree stem models, a case using LoD2 tree models, and a case using LoD3 tree models, respectively. $|U|_{ref}$ is the inflow

velocity magnitude at 1.75 m height, which is 2.88 m s^{-1} for the isolated tree and street canyon cases, and 3.68 m s^{-1} for the realistic urban geometry cases. As mentioned in Section 2.3.3, the values for $|U|_{ref}$ in the realistic urban geometry cases derive from a meteorological station located in the Noordereiland area. On the other hand, for the ideal cases, $|U|_{ref}$ was derived from past measurements recorded in the area and already used in our previous studies, as specified in Section 2.3.1. From our input velocity, we apply a logarithmic scaling to derive $|U|_{ref}$ at pedestrian height.

Note that in this work, the values of non-dimensional velocity magnitude differences are expressed as percentages.

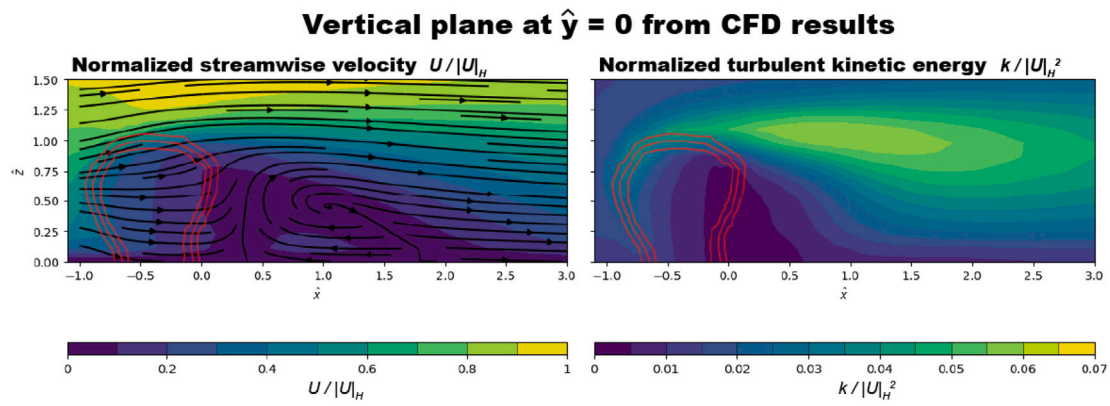
2.6. Verification and validation

Previous studies (Kang et al., 2020; Manickathan, 2019; Manickathan et al., 2018) have demonstrated the ability of numerical models to reproduce the wind velocity deficit due to trees by comparing CFD predictions with field and experimental measurements. For instance, Manickathan (2019) used a *Buxus sempervirens* plant for experimental measurements and has compared the results with CFD predictions to investigate the accuracy of the numerical model in predicting the mean airflow and the turbulence modification due to vegetation. We use this case to verify and validate our implementation.

The plant geometry used by Manickathan (2019) for their simulations (Fig. A.3) faithfully resembles the foliage outline (3D alpha shape) of the tested specimen; therefore, we would classify his model as LoD3 through visual inspection. The author also uses the same tree modeling approach as we do in Eq. (1) to Eq. (3). Thus, to verify and indirectly validate our implementation, we performed CFD simulations with the same plant model and settings as the author but using our implementation of $k - \epsilon$ turbulence model and OpenFOAM solver with added tree effects. To accomplish this task we used the same configuration used in Manickathan (2019), as well as the same tree geometry. All information regarding this set up can be found in Manickathan (2019), Chapter 7.

The comparison results displayed in Fig. 4 show that the CFD results using our implementation of $k - \epsilon$ turbulence model and OpenFOAM solver are consistent with those using the CFD model proposed by Manickathan (2019). This indicates that the tree numerical model we implemented is also valid and can predict results as accurate as the benchmark model. Based on the normalized velocity profile, the CFD predictions seem to always underestimate the peak wake velocity deficit at these three heights when compared to the experimental values. Manickathan (2019) believes that the underestimation is a result of using a porous media approximation for the tree model, which typically fails to accurately capture sharp velocity gradients, due to the lack of explicit modeling of the tree geometry. This also emphasizes the importance of using explicit trunk models in the LoD2 and LoD3 tree models we use in this paper.

The reason to perform the previous validation resides on the fact that no other wind tunnel measurements including trees was freely accessible to us for further comparison. In addition, to the best of our knowledge, experiments including different level of details in trees have yet to be completed, and therefore no available ground truth still exists. As such, one can fairly claim that the conclusions presented in this paper do have some uncertainty. For that, in order to minimize the impact of this uncertainty, this paper focuses on the general trends shown by different tree types and different urban morphologies, and avoids relying on the characteristics of a specific tree model or at a particular location. In this way, the conclusions drawn in this study remain well instructive — we are able to make a valid prediction of the effect of tree drags on wind and analyze the generic effect of tree LoDs from the comparison of a number of test cases. However, further studies that include measurements with trees are necessary to further support our conclusions.



Comparisons between CFD results and wind tunnel measurement

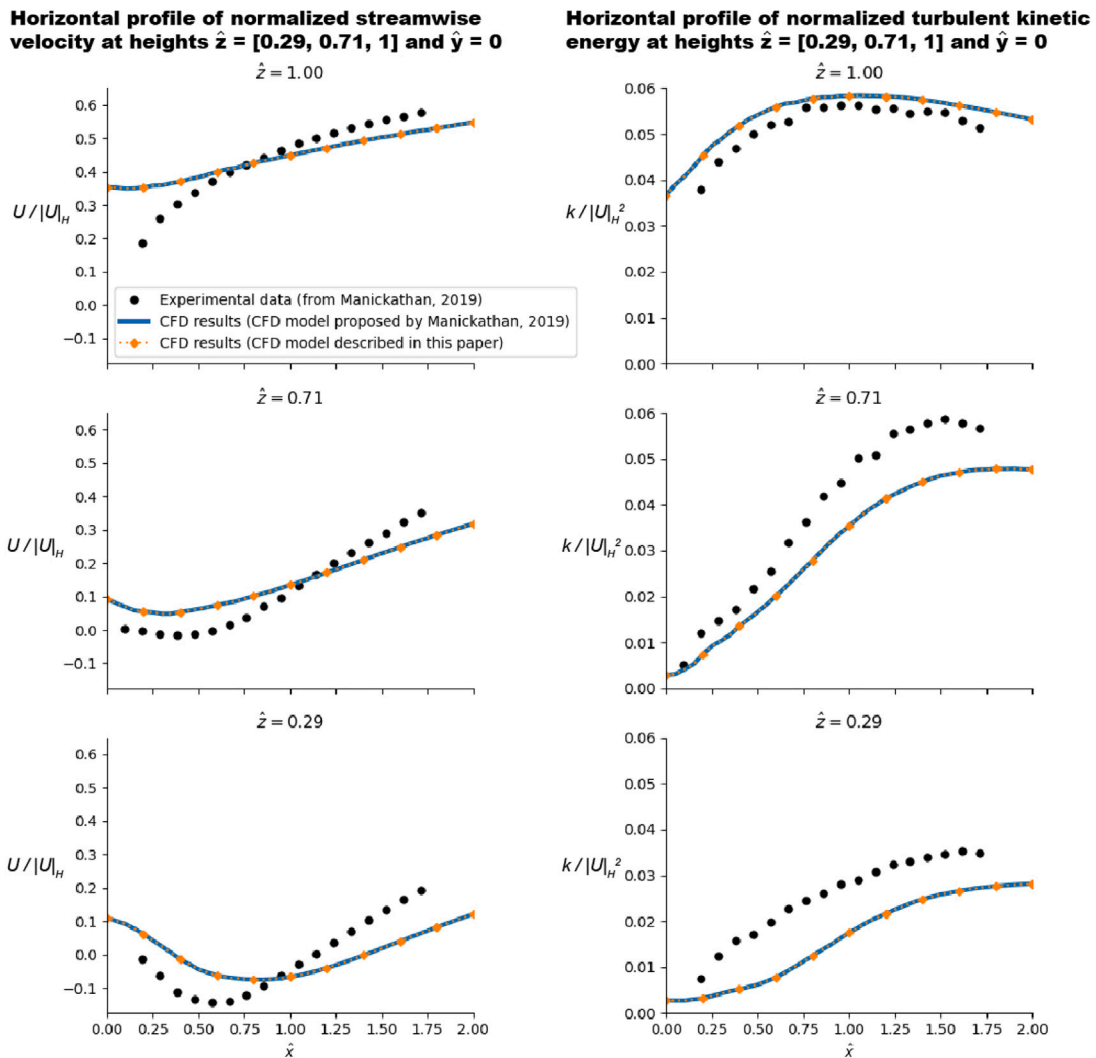


Fig. 4. Verification by comparing normalized velocity $U/|U|_H$ and turbulent kinetic energy $k/|U|_H^2$ at normalized heights $\hat{z} = [0.29, 0.71, 1]$. $|U|_H = 0.77 \text{ ms}^{-1}$ at $\hat{z} = 1$, which is the tree-canopy height velocity at normalized height $\hat{z} = 1$ used by Manickathan (2019).

3. Results

3.1. Isolated tree

The settings of all isolated tree test cases are summarized in Table 3. For each test case, the same value of the tree LAD is used: $2.2 \text{ m}^2 \text{ m}^{-3}$.

Fig. 5 shows the vertical contours of the non-dimensional velocity magnitude predictions for the isolated tree cases, and the horizontal contours at pedestrian height (1.75 m) are shown in Fig. 6. Note the ranges of these contours are cropped to focus on the wind velocity difference around and within the tree models. The white lines indicate the outlines of the tree models.

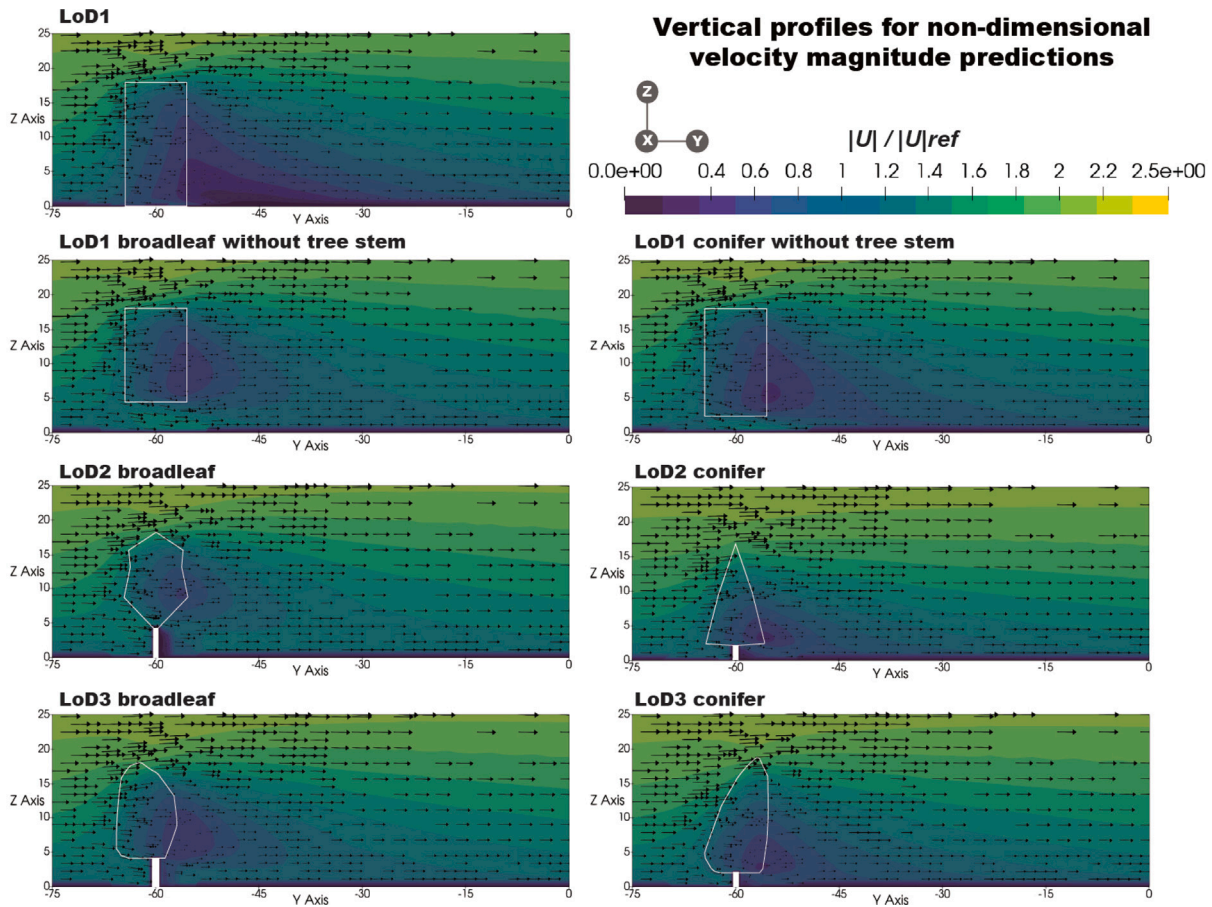


Fig. 5. Vertical contours for non-dimensional velocity magnitude predictions at middle plane in XY. $|U|_{ref} = 2.88 \text{ m s}^{-1}$.

Table 3
Settings of isolated tree test cases.

Case ID	Tree LoD	Tree type	LAD value ($\text{m}^2 \text{m}^{-3}$)
1	LoD1	–	2.2
1'	LoD1 without tree stem	Broadleaf	
1''	LoD1 without tree stem	Conifer	
2	LoD2	Broadleaf	
3	LoD3		
4	LoD2	Conifer	
5	LoD3		

From Fig. 5, we can see clear differences between the non-dimensional velocity magnitude predictions around the LoD1 tree model with the predictions around the LoD2 and LoD3 tree models. The recirculation zone in LoD1 is closer to the ground than in Cases 2–5. Fig. 6 also further shows that compared to the LoD2 or LoD3 tree models, the LoD1 tree model has a greater reduction effect on the downstream wind speed, creating a larger area with wind speeds less than 1 m s^{-1} at pedestrian height. This is somewhat expected since it is related to the fact that the LoD1 tree model have a larger cross-sectional area at the height of 1.75 m than the LoD2 or LoD3 tree models, where only the stem is present. We can also find that compared to LoD2 or LoD3 broadleaf tree models, the recirculation zones of LoD2 and LoD3 conifer tree models are closer to the ground, resulting in a slower downstream wind speed at pedestrian height. This largely derives from the fact that conifer tree models have shorter stems. Therefore, to improve the accuracy of wind environment simulation results, the type of tree models should be chosen as close as possible to reality and it is

best not to assume that all trees in the study area have the same type or shape.

To better investigate the impact of tree LoDs on velocity magnitude predictions, the five test cases (Table 3) are compared in pairs to get C_{11-12} , C_{12-11}^* and C_{12-13} . For instance, the velocity magnitude prediction of case 2 is subtracted from that of case 1 and then normalized by $|U|_{ref}$ (2.88 m s^{-1}), so that we can obtain the non-dimensional velocity magnitude difference between the case with a LoD1 tree model and the case with a LoD2 broadleaf tree model. The results are shown in Fig. 7.

Clearly, the velocity magnitude difference between LoD1 and LoD2 (C_{11-12}) is much greater than the difference between LoD2 and LoD3 (C_{12-13}), regardless of broadleaf or conifer. This is specially highlighted with the strict LoD1 definition where the porous tree reaches the ground. This effect is reduced when no tree stem is considered with LoD1, appearing an important difference around the tree stem due to its inexistence in LoD1, compared to LoD2. The overall mean and standard deviation difference is much larger when we compare LoD1 and higher LoDs. However, when the tree is not extended till the ground, the mean difference is similar to those encountered for LoD2 and LoD3, while the standard deviation remains larger for LoD1. It is nevertheless important to mention that still local large differences can be encountered due to diverse shapes of tree stems, as it can be seen in C_{12-13} for broadleaf tree. This might be relevant depending of the zone of interest in our simulation results.

3.1.1. Idealized street canyon

To further generalize the tree LoD impact in urban flow simulations we explore their effect in an idealized street canyon with perpendicular and parallel wind directions (Fig. 2). The settings of all street canyon test cases are summarized in Table 4. Similar to isolated tree cases,

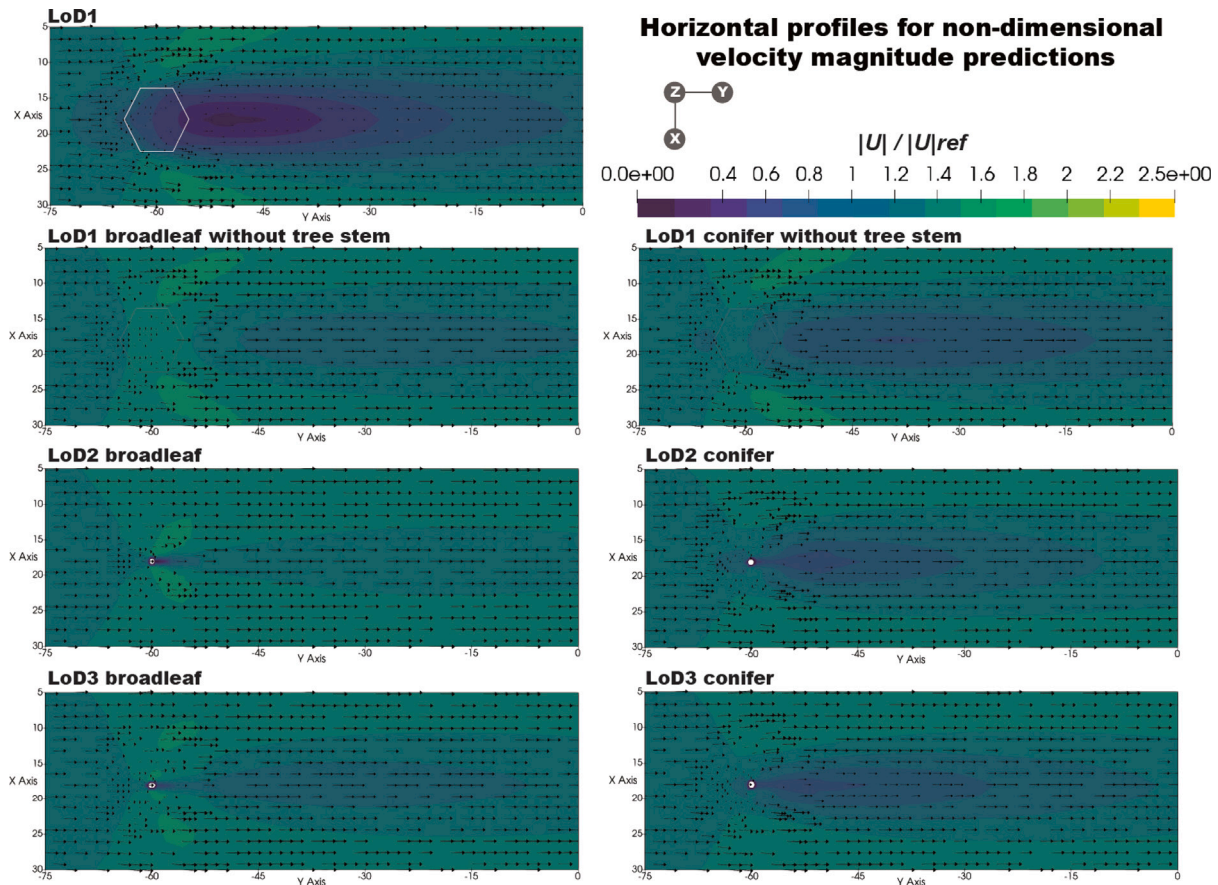


Fig. 6. Horizontal contours at pedestrian height (1.75 m) for non-dimensional velocity magnitude predictions. $|U|_{ref} = 2.88 \text{ m s}^{-1}$.

Table 4
Settings of street canyon test cases.

Case ID	Inflow direction	Tree LoD	Tree type	LAD value ($\text{m}^2 \text{m}^{-3}$)
6	Perpendicular to buildings	LoD1	–	0.2
6'		LoD1 without tree stem	Broadleaf	
6''		LoD1 without tree stem	Conifer	
7		LoD2	Broadleaf	
8		LoD3	Broadleaf	
9		LoD2	Conifer	
10	LoD3	Conifer	1.0	
11	Parallel to buildings	LoD1	–	1.4
11'		LoD1 without tree stem	Broadleaf	
11''		LoD1 without tree stem	Conifer	
12		LoD2	Broadleaf	
13		LoD3	Broadleaf	
14		LoD2	Conifer	
15	LoD3	Conifer	2.2	

these street canyon cases are compared in pairs to obtain the non-dimensional velocity magnitude difference (C_{I2-11} , C_{I2-11}^* and C_{I2-13}). $|U|_{ref}$ is 2.88 m s^{-1} .

Figs. 8 and 9 present same example plots of C_{I2-11} , C_{I2-11}^* and C_{I2-13} for street canyon cases with broadleaf tree models. As it can be seen, differences with LoD1 still remain remarkably larger than higher LoDs, which is expected at pedestrian height. These differences in the mean are reduced when an LoD1 without tree stem is used, however the standard deviation remains much higher than that for LoD2 and LoD3 differences. This can also be observed in the contours plots, with wider color changes. Comparing Figs. 8 and 9 it is also clear that a parallel wind direction, compared to a perpendicular wind direction, results in higher C_{I2-11} (over 50% at most areas) and C_{I2-13} values (around 5% to

25% at most areas), i.e., greater wind velocity variation due to tree LoD changes. This is likely related to the fact that a parallel wind direction leads to higher wind speeds within the street canyon. Therefore, areas with higher local wind speeds may have a greater need for tree models with higher LoDs to provide more realistic predictions.

Since different LAD values may also impact the simulations, we analyzed the fourteen cases listed in Table 4 with changing LAD values as follows: 0.2, 0.6, 1.0, 1.4, 1.8 and $2.2 \text{ m}^2 \text{m}^{-3}$. This results in 72 plots of non-dimensional velocity magnitude difference (C_{I2-11} , C_{I2-11}^* and C_{I2-13}) in total. For the sake of brevity, not all plots are shown in this paper, but the 12 plots generated using broadleaf cases with LAD = 0.2 and $2.2 \text{ m}^2 \text{m}^{-3}$ are shown in Figs. 8 and 9 to illustrate the impact of LAD. The corresponding 12 plots generated using conifer

Non-dimensional velocity magnitude difference

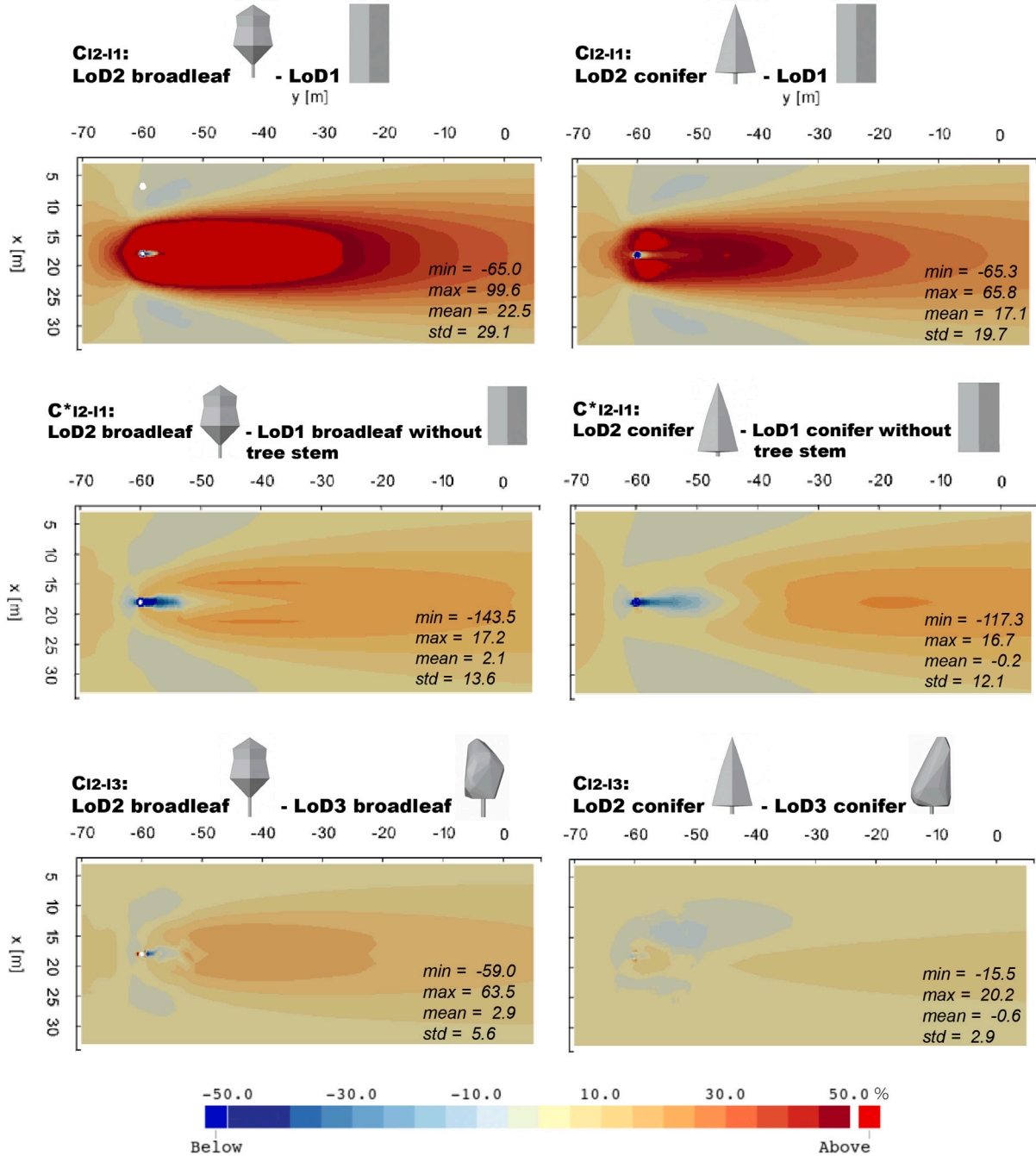


Fig. 7. Non-dimensional velocity magnitude difference contours at pedestrian height (1.75 m) for isolated tree cases; The ‘min’, ‘max’, ‘mean’, ‘std’ refer to the minimum, maximum, average and standard deviation values of non-dimensional velocity magnitude differences, respectively.

cases with LAD = 0.2 and 2.2 m²m⁻³ can be found in Figs. A.4 and A.5 in Appendix.

When comparing subplots 1 and 2, 3 and 4, or 5 and 6 in Figs. 8 and 9, it seems that higher LAD may lead to higher values of non-dimensional velocity magnitude difference (C_{12-11} and C_{12-13}). However, the differences between them are difficult to distinguish clearly

with the naked eye and need to be described in a more quantitative way.

Thus, we compare the differences of all 72 non-dimensional velocity magnitude difference plots in terms of the mean values and 95% confidence intervals, which were statistically derived from data measured at pedestrian height (1.75 m). The results are shown in Fig. 10. There are a few conclusions that can be drawn from this figure:

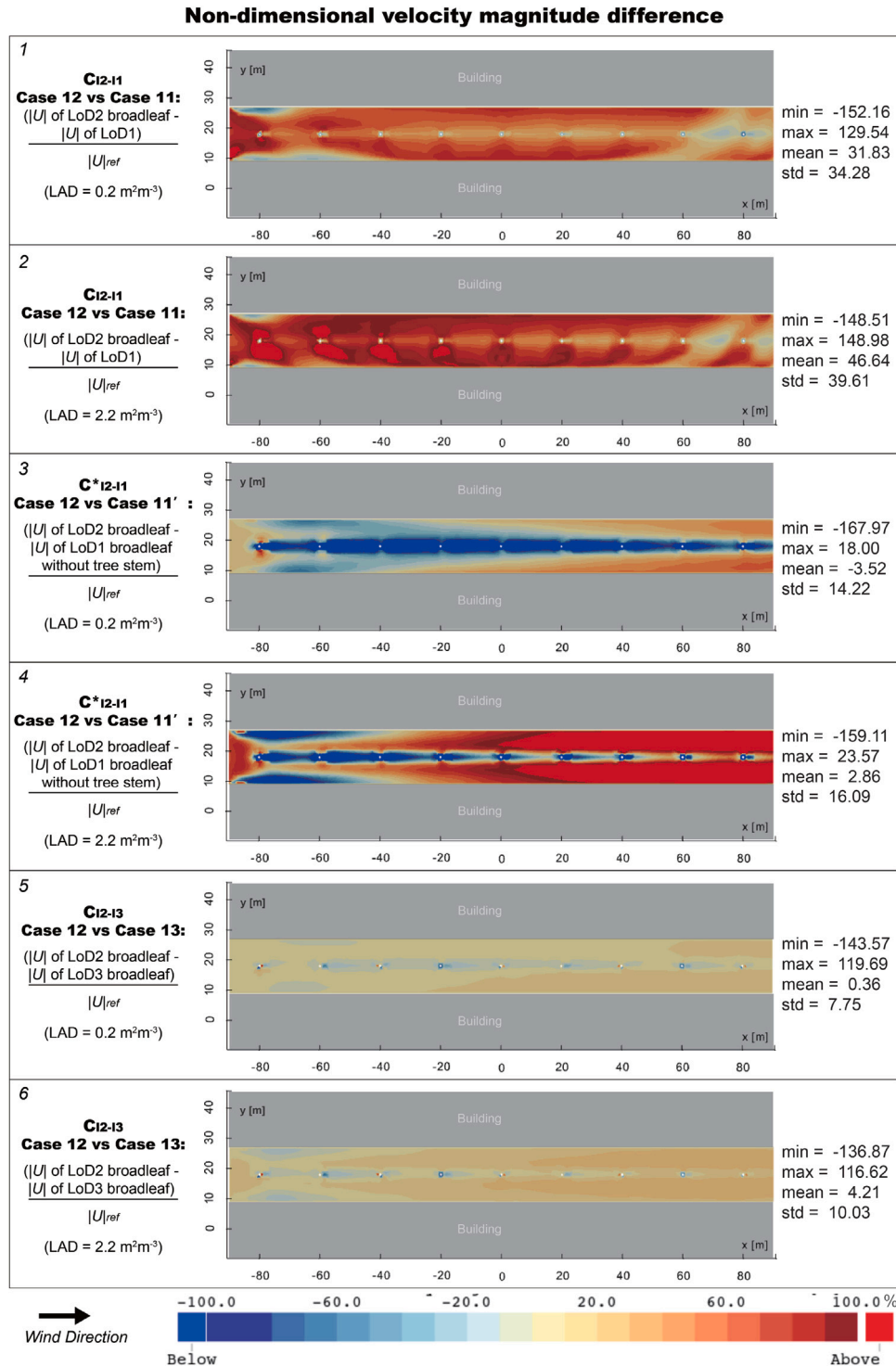


Fig. 9. Contours for the non-dimensional velocity magnitude difference at pedestrian height (1.75 m) for street canyon cases with a parallel wind direction. Case 11: LoD1 tree models; Case 11': LoD1 broadleaf tree models without tree stems; Case 12: LoD2 broadleaf tree models; Case 13: LoD3 broadleaf tree models; $|U|_{ref} = 2.88 \text{ m s}^{-1}$. Note: Since the parallel wind brings higher values of non-dimensional velocity magnitude difference, the colormap of [-15-15] used in Fig. 8 is not enough to clearly show the difference between subplots, so the range of colormap here is [-100-100]. (For interpretation of the references to color in this figure legend, the reader is referred to the web version of this article.)

4. The flow wind direction has a major role in the impact of tree LoDs, resulting in larger velocity differences for the parallel canyon flow than the perpendicular one.
5. The values of C_{12-13} for conifer cases are overall lower than in broadleaf cases. This might be related to the geometry of tree

canopy. We can see from Fig. 1 that the canopies of conifer trees are wider in the bottom (near the pedestrian height), which could reduce the local wind speed and thus result in less velocity differences due to tree LoD difference.

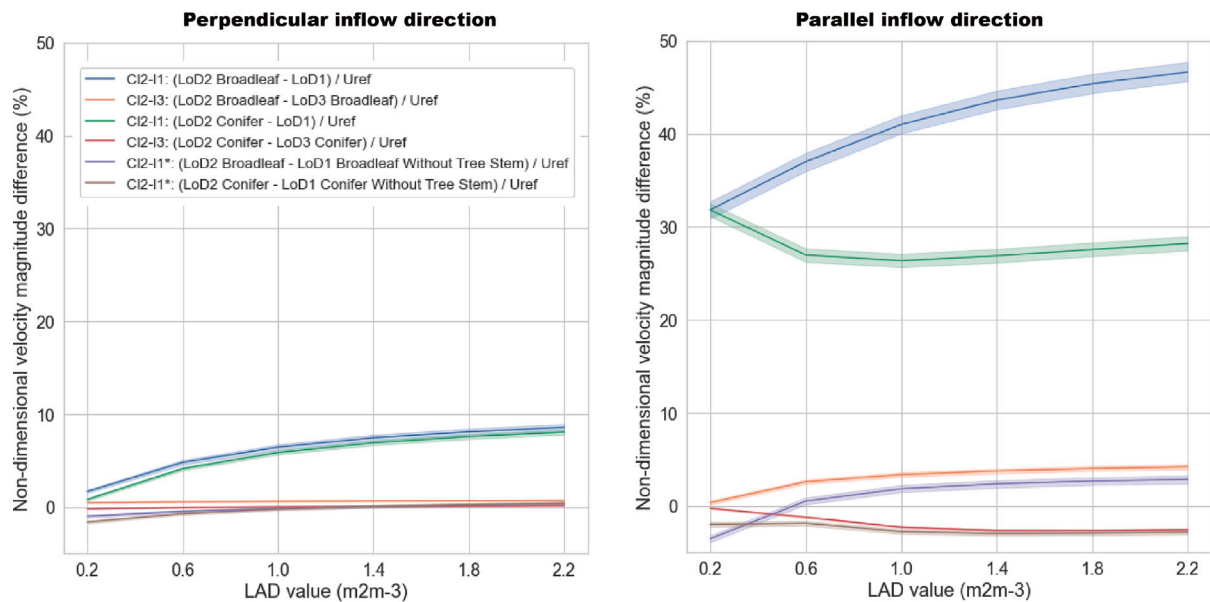


Fig. 10. Mean values and 95% confidence interval of the non-dimensional velocity magnitude difference measured at pedestrian height (1.75 m) for street canyon cases.

Table 5
Settings of realistic urban geometry test cases.

Case ID	Tree LoD	LAD value (m ² m ⁻³)
16	LoD1	Broadleaf: 1.6;
17	LoD2	
18	LoD3	Conifer: 1.4;

3.1.2. Realistic urban geometry

The settings of realistic urban geometry test cases are summarized in Table 5. The LAD values for broadleaf trees and conifer trees are 1.6 and 1.4 m² m⁻³, respectively, which are consistent with those used in Lalic and Mihailovic (2004). Also, according to the findings in Section 3.1.1, they are sensitive enough to ensure a relatively large and stable velocity magnitude differences as they are greater than 1.4 m² m⁻³.

The non-dimensional velocity magnitude differences measured at pedestrian height are presented in Fig. 11. Note that compared to the isolated tree cases and the street canyon cases, the $|U|_{ref}$ used for the realistic urban geometry test cases is 3.68 m s⁻¹, which is estimated based on open datasets as described in Section 2.3.3. We can find that there are obvious differences between the LoD1 case (Case 16) and LoD2 case (Case 17). At some dense-tree areas and in some narrow passages between buildings, i.e. in the street canyons, the velocity magnitude differences are over 1.0 m/s ($|U|_{ref} * 30\%$). However, only slight differences (around -5% to 5% at most places, i.e. lower than 0.2 m/s) between LoD2 case (Case 17) and LoD3 case (Case 18) are found. This is further supported by the mean and standard deviation differences over the domain. Thus, focusing on the mean values it may be good enough in principle to have the LoD2 tree model for wind environment studies in the Noordereiland region.

Nevertheless, it is important to mention that similarly to the single tree and the street canyon analysis, maximum and minimum difference values between higher LoDs can be large also locally. In Fig. 11 this occurs in specific street canyons, that might change with wind direction in our simulations. Therefore, for specific urban improvements in localized street areas we recommend that several analysis are completed

prior modifications. Those analysis should not only include higher LoD for trees, but they should also encompass different wind directions that are plausible within the area of interest.

4. Conclusions

In this paper we numerically analyzed the effects of tree LoDs on wind predictions. We address this by comparing the non-dimensional velocity magnitude differences between simulations with LoD1, LoD2, or LoD3 tree models. To further understand these differences in changing environmental contexts we use three morphologies: an isolated tree, an idealized street canyon (with perpendicular and parallel wind), and a real urban scenario in Rotterdam, The Netherlands. Understanding differences in wind speed when including tree geometries in urban flow simulations can guide urban development decisions that minimize computational and time resources while maximizing flow predictability.

One of the main conclusions is that the non-dimensional velocity magnitude differences with LoD1 tree models (with porous stem) are remarkably larger than those with higher LoDs. For the Noordereiland cases, the velocity magnitude differences between the case 16 (with LoD1 tree models) and 17 (with LoD2 tree models) can be over 1.0 m/s while the differences between the case 17 and 18 (with LoD3 tree models) are lower than 0.2 m/s. A similar pattern can be found in the test cases of isolated tree and street canyon. This result is somewhat expected and directly derives from the fact that the LoD1 model does not include a tree stem, but the same porous zone used for the crown. As our results show, including removing the porous part of the tree where the tree stem is supposed to be can limit these differences considerably. Nevertheless, since the differences found in wind predictions by using low LoD tree models (even when removing the stem porous part) are non-negligible, researchers should take them into account when comparing their results with local measurements or wind tunnel data that include vegetation elements.

An additional conclusion that can be derived directly from the previous argument is that including a realistic tree stem is also an important feature that should not be ignored. Even when using LoD1

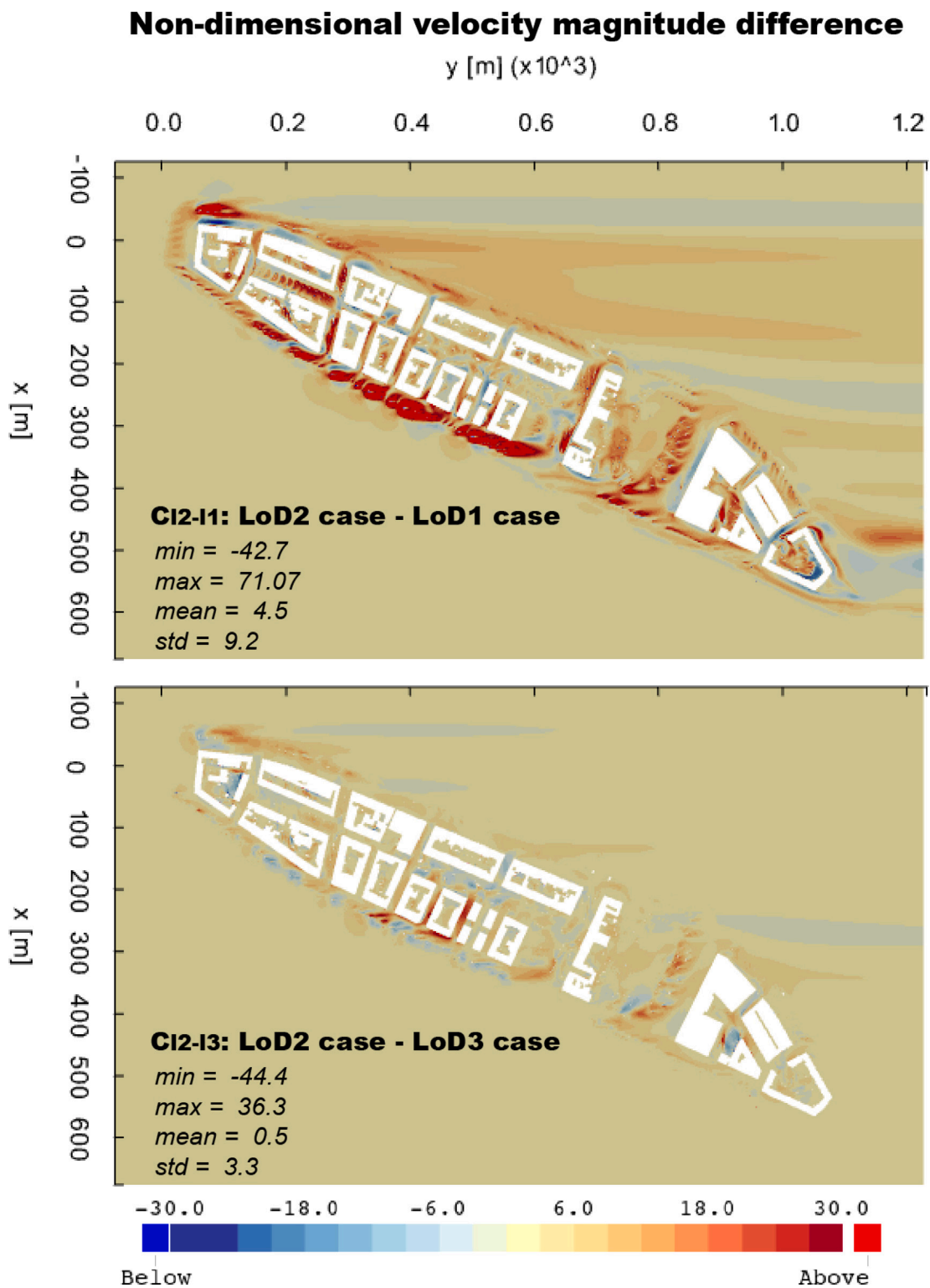


Fig. 11. Non-dimensional velocity magnitude difference measured at pedestrian height (1.75 m) for urban geometry cases; The 'min', 'max', 'mean', 'std' refer to the minimum, maximum, average and standard deviation values of non-dimensional velocity magnitude differences, respectively.

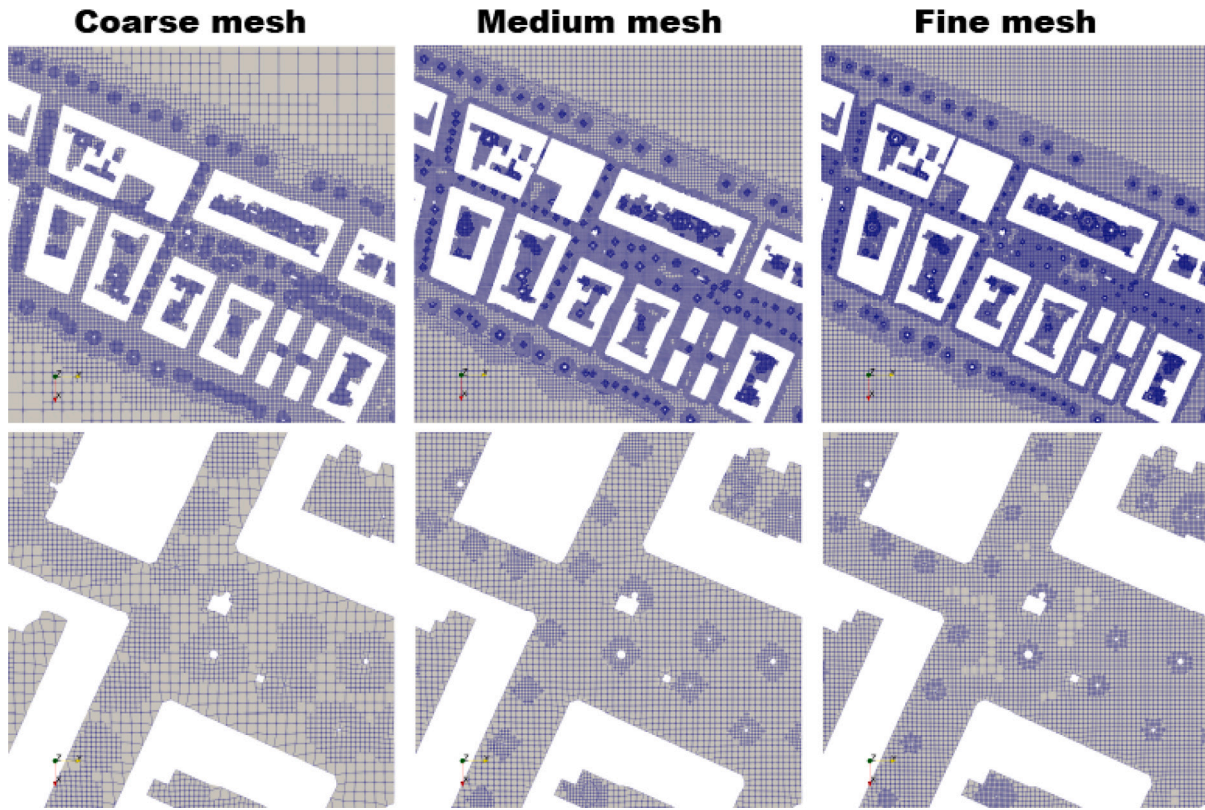
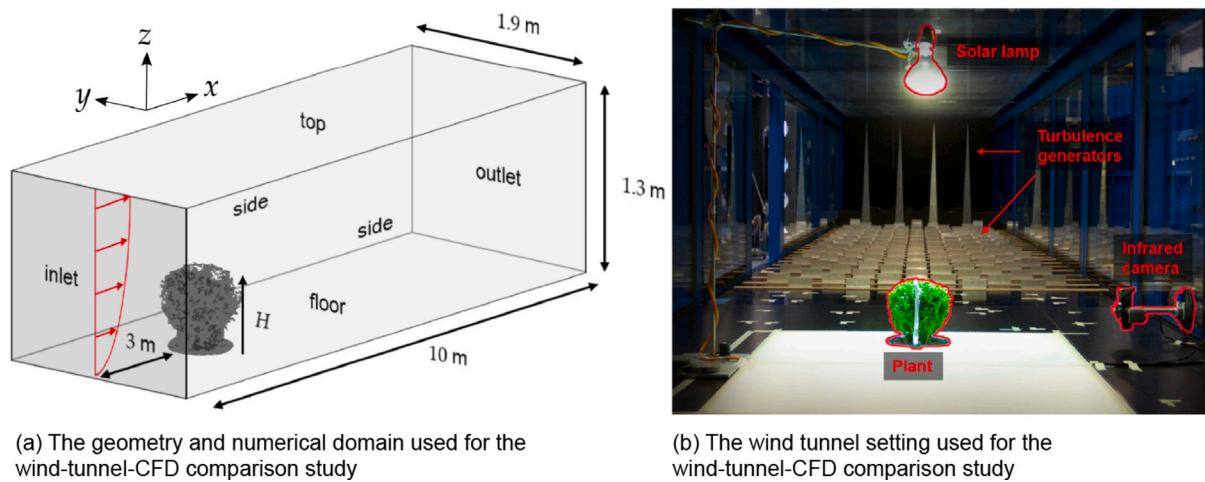


Fig. A.1. Meshes with different resolutions.



Fig. A.2. Probes used to compute grid convergence index. Grey: buildings, green: trees, red: probes. (For interpretation of the references to color in this figure legend, the reader is referred to the web version of this article.)

The modeled geometry and wind tunnel setting used by Lento Manickathan



(a) The geometry and numerical domain used for the wind-tunnel-CFD comparison study

(b) The wind tunnel setting used for the wind-tunnel-CFD comparison study

Fig. A.3. The simulated plant geometry and the wind tunnel setting used by Lento Manickathan for the wind-tunnel-CFD comparison study. The plant-canopy height $H = 0.21$ m (not to scale).

Source: Adapted from Manickathan (2019).

trees without tree stem, the differences in mean were similar to those encountered for higher LoD models, but with much larger standard deviations within the domain. This might be related to the fact that no tree stem was present, and therefore the differences in the flow were much larger at the pedestrian height allowing the flow to develop downstream in different patterns than those encountered between LoD2 and LoD3 differences.

Instead, when using tree models in higher LoD (LoD2 or LoD3 levels) the differences found for wind predictions in urban areas were rather limited, and therefore less of a concern for researchers when comparing with ground truth data. These differences are directly connected to the tree shape, and therefore depending on the height of the crown might have less of an impact towards pedestrians.

Regarding the effect of the tree species used within the study, we find that the values of C_{l2-l3} for conifer cases are overall lower than broadleaf cases. This might be explained by the small differences in shape between LoD2 and LoD3 for conifer trees, since the overall area above the tree stem is fairly the same. Nevertheless, this highlights the important role that the tree shape may play in the development of wind patterns in urban areas, and how the assumption that all trees within a study area have the same shape might not be the best approach.

Additionally, it can be concluded that tree LAD values and wind directions have a major role in the impact of tree LoDs. Generally, the larger the LAD value, the greater the velocity differences due to tree LoD variation, especially when the LAD is lower than $1.4 \text{ m}^2 \text{ m}^{-3}$. Similarly, larger velocity differences can be seen for the parallel canyon flow than the perpendicular flow, as the former one can provide a higher wind speed in the study area. Thus, for specific urban improvements in localized street areas, we recommend considering not only the shape of the trees and the higher LoD, but also the LAD of the trees and the most probable wind conditions in the area.

Lastly, a major point of this research is driven by our capability to reconstruct and introduce the tree elements within our simulations. The time cost to create geometries at LoD1, LoD2, or LoD3 with our approach is the same, however as it was shown in Table 1, the time spent to complete our simulations was largely different. Completing a simulation with LoD2/LoD3 level trees was approximately 2.5 times more costly than performing the simulation with LoD1 (with or without the tree stem). This suggests that during the design phase, where

multiple evaluations are needed, it might be more efficient to use simpler tree models, such as LoD1 without tree stems. However, once a final design is chosen, it is better to use more detailed models, like LoD2 or LoD3, for the prediction phase.

CRediT authorship contribution statement

Runnan Fu: Conceptualization, Data curation, Formal analysis, Investigation, Methodology, Software, Validation, Visualization, Writing – original draft. **Ivan Pađen:** Software, Supervision, Writing – review & editing, Conceptualization, Methodology, Project administration, Validation. **Clara García-Sánchez:** Conceptualization, Methodology, Project administration, Resources, Software, Supervision, Writing – review & editing.

Declaration of competing interest

The authors declare that they have no known competing financial interests or personal relationships that could have appeared to influence the work reported in this paper.

Data availability

Program language: C++, Python Software required: OpenFOAM, version 7 (The OpenFOAM Foundation, 2021). The source codes are available for downloading at the link: https://github.com/furunnan/Tree_Topo_Effects_on_Wind.

Acknowledgments

The authors would like to acknowledge Lento Manickathan for providing the tree models and CFD from Manickathan (2019), which helped us to complete the validation of our numerical model.

Appendix. Supplementary figures

See Figs. A.1–A.10.

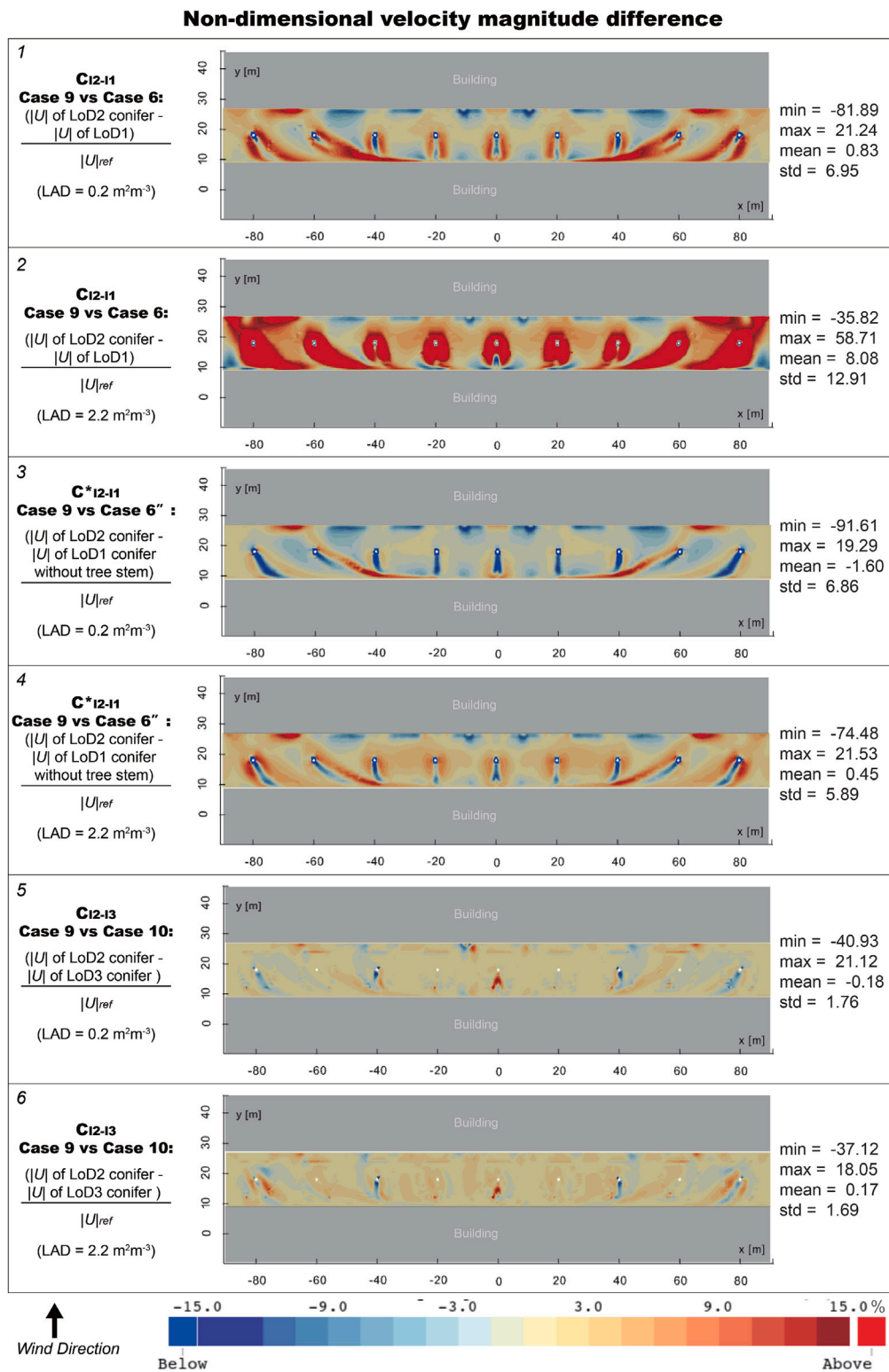


Fig. A.4. Contours for the non-dimensional velocity magnitude difference at pedestrian height (1.75 m) for street canyon cases with a perpendicular wind direction. Case 6: LoD1 tree models; Case 6": LoD1 conifer tree models without tree stems; Case 9: LoD2 conifer tree models; Case 10: LoD3 conifer tree models; $|U|_{ref} = 2.88 m s^{-1}$.

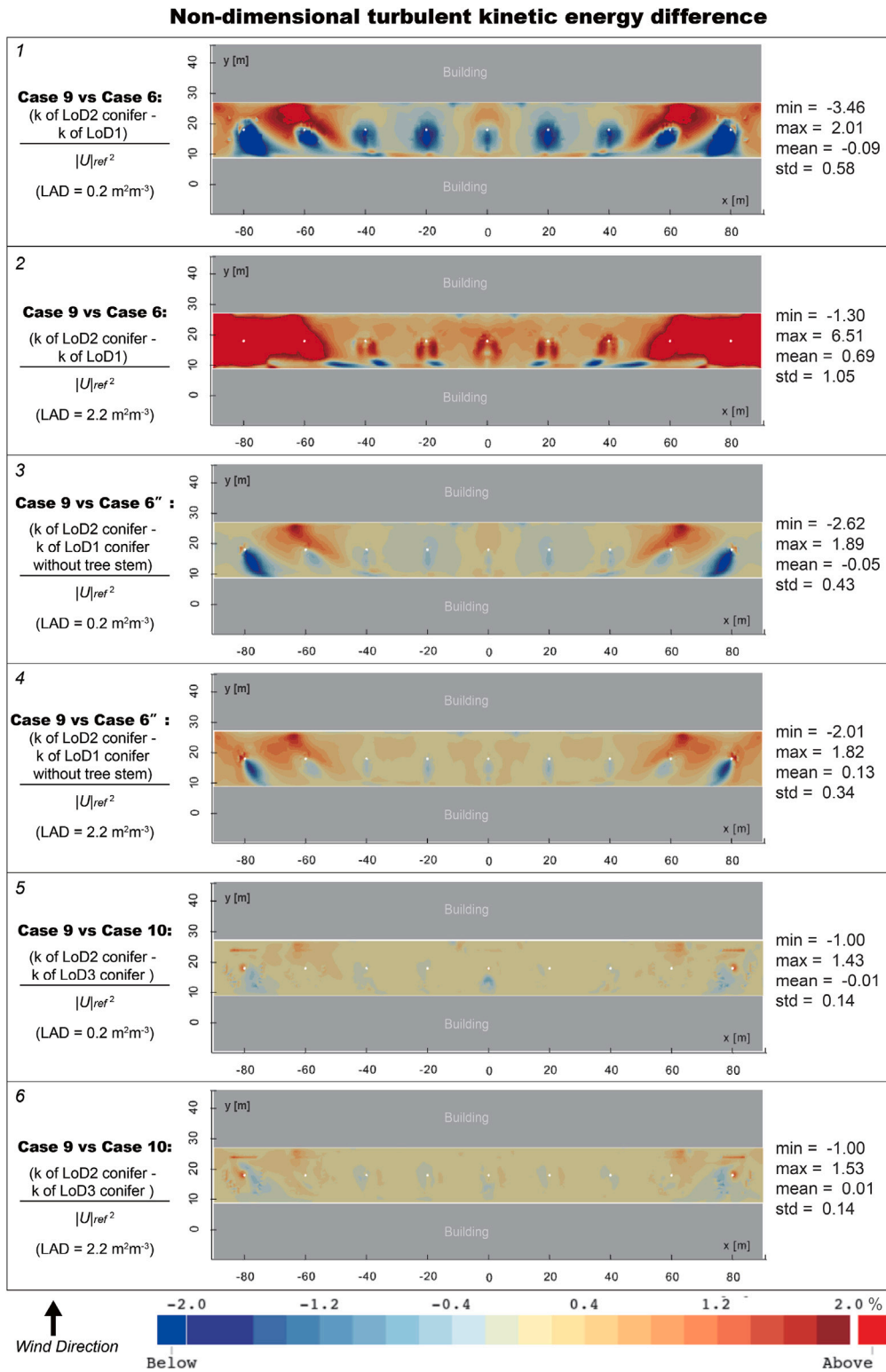


Fig. A.7. Contours for the non-dimensional turbulent kinetic energy difference at pedestrian height (1.75 m) for street canyon cases with a perpendicular wind direction. Case 6: LoD1 tree models; Case 6": LoD1 conifer tree models without tree stems; Case 9: LoD2 conifer tree models; Case 10: LoD3 conifer tree models; $|U_{ref}| = 2.88 \text{ m s}^{-1}$.

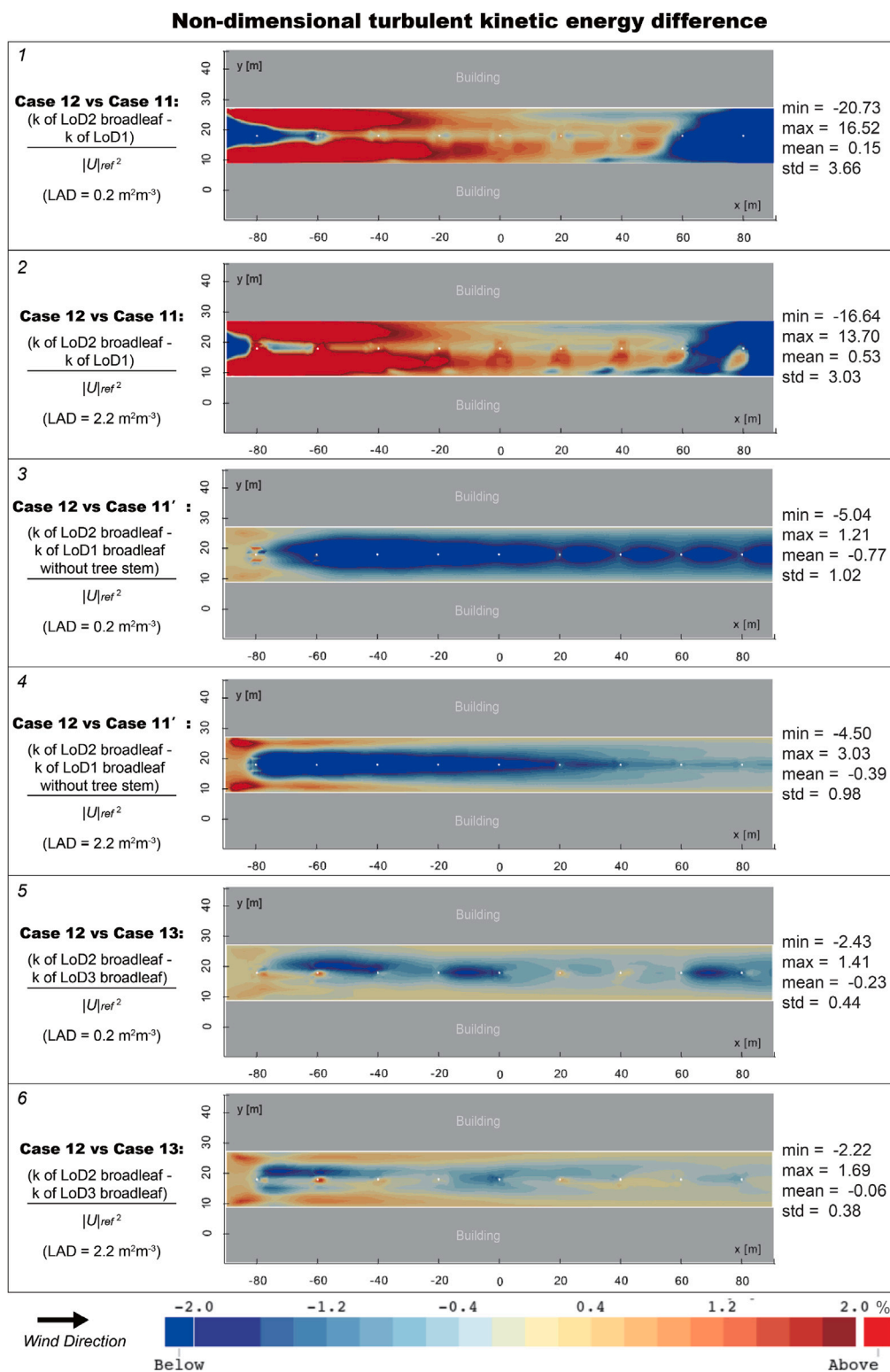


Fig. A.8. Contours for the non-dimensional turbulent kinetic energy difference at pedestrian height (1.75 m) for street canyon cases with a parallel wind direction. Case 11: LoD1 tree models; Case 11': LoD1 broadleaf tree models without tree stems; Case 12: LoD2 broadleaf tree models; Case 13: LoD3 broadleaf tree models; $|U_{ref}| = 2.88 \text{ m s}^{-1}$.

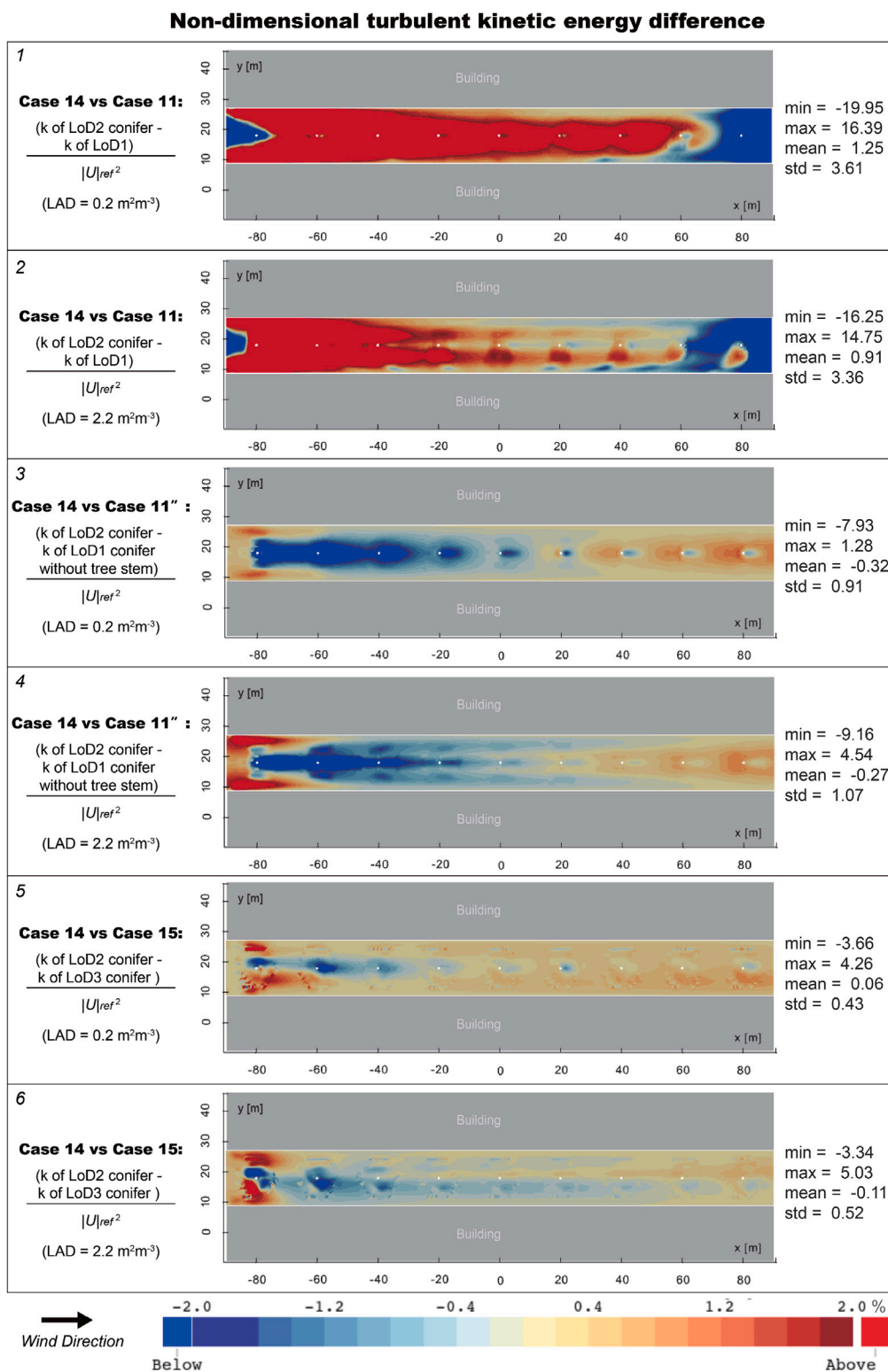


Fig. A.9. Contours for the non-dimensional turbulent kinetic energy difference at pedestrian height (1.75 m) for street canyon cases with a parallel wind direction. Case 11: LoD1 tree models; Case 11": LoD1 conifer tree models without tree stems; Case 14: LoD2 conifer tree models; Case 15: LoD3 conifer tree models; $|U_{ref}| = 2.88 \text{ m s}^{-1}$.

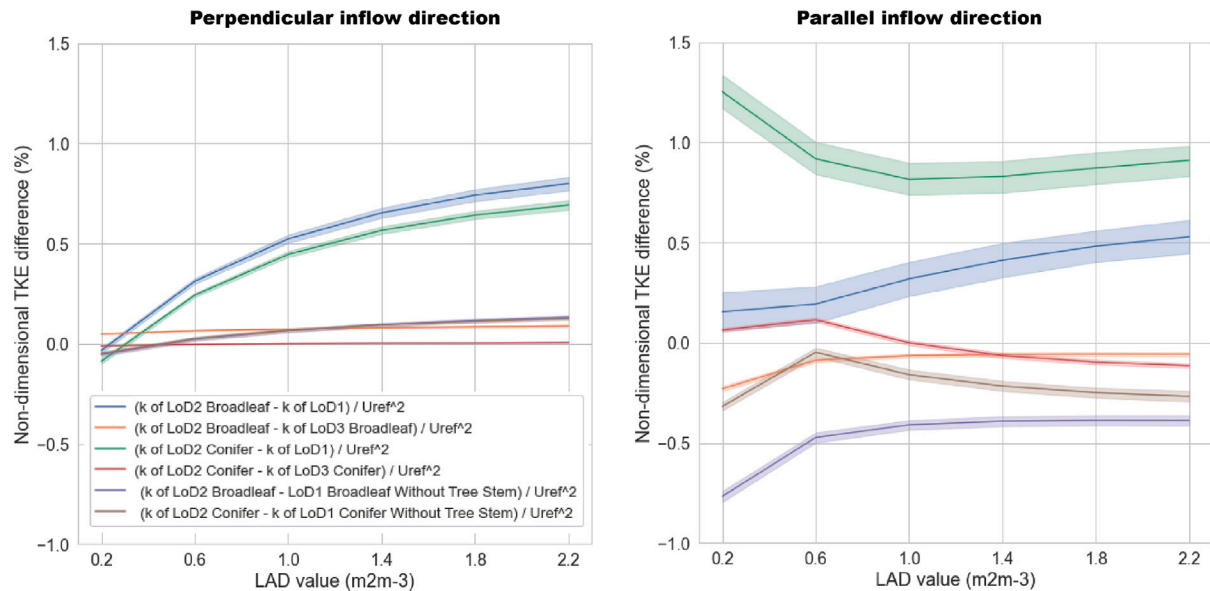


Fig. A.10. Mean values and 95% confidence interval of the non-dimensional turbulent kinetic energy difference measured at pedestrian height (1.75 m) for street canyon cases.

References

- Aflaki, A., Mirnezhad, M., Ghaffarianhoseini, A., Ghaffarianhoseini, A., Omrany, H., Wang, Z. H., & Akbari, H. (2017). Urban heat island mitigation strategies: A state-of-the-art review on Kuala Lumpur, Singapore and Hong Kong. *Cities*, 62, 131–145. <http://dx.doi.org/10.1016/J.CITIES.2016.09.003>.
- Amorim, J. H., Rodrigues, V., Tavares, R., Valente, J., & Borrego, C. (2013). CFD modelling of the aerodynamic effect of trees on urban air pollution dispersion. *Science of the Total Environment*, 461–462, 541–551. <http://dx.doi.org/10.1016/j.scitotenv.2013.05.031>.
- Balczó, M., Gromke, C., & Ruck, B. (2009). Numerical modeling of flow and pollutant dispersion in street canyons with tree planting. *Meteorologische Zeitschrift*, 18(2), 197–206. <http://dx.doi.org/10.1127/0941-2948/2009/0361>.
- Biljecki, F., Ledoux, H., & Stoter, J. (2016). An improved LOD specification for 3D building models. *Computers, Environment and Urban Systems*, 59, 25–37.
- Blocken, B. (2015). Computational Fluid Dynamics for urban physics: Importance, scales, possibilities, limitations and ten tips and tricks towards accurate and reliable simulations. *Building and Environment*, 91, 219–245. <http://dx.doi.org/10.1016/J.BUILDENV.2015.02.015>.
- Blocken, B., Janssen, W. D., & van Hooff, T. (2012). CFD simulation for pedestrian wind comfort and wind safety in urban areas: General decision framework and case study for the Eindhoven University campus. *Environmental Modelling & Software*, 30, 15–34. <http://dx.doi.org/10.1016/J.ENVSOFT.2011.11.009>.
- Brozovsky, J., Radivojevic, J., & Simonsen, A. (2022). Assessing the impact of urban microclimate on building energy demand by coupling CFD and building performance simulation. *Journal of Building Engineering*, 55, <http://dx.doi.org/10.1016/j.jobee.2022.104681>.
- Brozovsky, J., Simonsen, A., & Gaitani, N. (2021). Validation of a CFD model for the evaluation of urban microclimate at high latitudes: A case study in Trondheim, Norway. *Building and Environment*, 205, <http://dx.doi.org/10.1016/j.buildenv.2021.108175>.
- Buccolieri, R., Santiago, J. L., Rivas, E., & Sanchez, B. (2018). Review on urban tree modelling in CFD simulations: Aerodynamic, deposition and thermal effects. *Urban Forestry & Urban Greening*, 31, 212–220. <http://dx.doi.org/10.1016/J.UFUG.2018.03.003>.
- Celik, I. B., Ghia, U., Roache, P. J., Freitas, C. J., Coleman, H., & Raad, P. E. (2008). Procedure for estimation and reporting of uncertainty due to discretization in CFD applications. *Journal of Fluids Engineering, Transactions of the ASME*, 130, <http://dx.doi.org/10.1115/1.2960953>.
- Chen, M. (2013). Comparison of 3D tree parameters. (Master Thesis), Wageningen University.
- Fouillet, A., Rey, G., Laurent, F., Pavillon, G., Bellec, S., Guihenneuc-Jouyaux, C., Clavel, J., Jouglu, E., & Hémon, D. (2006). Excess mortality related to the August 2003 heat wave in France. *International Archives of Occupational and Environmental Health*, 80(1), 16–24. <http://dx.doi.org/10.1007/S00420-006-0089-4>, URL https://www.researchgate.net/publication/7255542_Excess_Mortality_Related_to_the_August_2003_Heat_Wave_in_France.
- Franke, J., Hellsten, A., Schlunzen, K. H., & Carissimo, B. (2011). The COST 732 Best Practice Guideline for CFD simulation of flows in the urban environment: a summary. *International Journal of Environment and Pollution*, 44(1–4), 419–427. <http://dx.doi.org/10.1504/IJEP.2011.038443>, URL <https://www.inderscienceonline.com/doi/abs/10.1504/IJEP.2011.038443>.
- García-Sánchez, C., Vitalis, S., Paden, I., & Stoter, J. (2021). The impact of level of detail in 3d city models for cfd-based wind flow simulations. *International Archives of the Photogrammetry, Remote Sensing and Spatial Information Sciences - ISPRS Archives*, 46(4/W4-2021), 67–72. <http://dx.doi.org/10.5194/ISPRS-ARCHIVES-XLVI-4-W4-2021-67-2021>, URL <https://research.tudelft.nl/en/publications/the-impact-of-level-of-detail-in-3d-city-models-for-cfd-based-win>.
- Gromke, C., Blocken, B., Janssen, W., Merema, B., van Hooff, T., & Timmermans, H. (2015). CFD analysis of transpirational cooling by vegetation: Case study for specific meteorological conditions during a heat wave in Arnhem, Netherlands. *Building and Environment*, 83, 11–26. <http://dx.doi.org/10.1016/J.BUILDENV.2014.04.022>.
- Gromke, C., Ruck, B., Gromke, C., & Ruck, B. (2012). Pollutant concentrations in street canyons of different aspect ratio with avenues of trees for various wind directions. *Boundary-Layer Meteorology*, 144(1), 41–64. <http://dx.doi.org/10.1007/S10546-012-9703-Z>, URL <https://link.springer.com.tudelft.idm.oclc.org/article/10.1007/s10546-012-9703-z>.
- de Groot, R. (2020). Automatic construction of 3D tree models in multiple levels of detail from airborne LiDAR data. URL <https://repository.tudelft.nl/islandora/object/uuid%3A3e169fc7-5336-4742-ab9b-18c158637cfe>.
- Hefny Salim, M., Heinke Schliinzen, K., & Grawe, D. (2015). Including trees in the numerical simulations of the wind flow in urban areas: Should we care? *Journal of Wind Engineering and Industrial Aerodynamics*, 144, 84–95. <http://dx.doi.org/10.1016/J.JWEIA.2015.05.004>, URL https://www.researchgate.net/publication/281102280_Including_trees_in_the_numerical_simulations_of_the_wind_flow_in_urban_areas_Should_we_care.
- Hong, B., & Lin, B. (2015). Numerical studies of the outdoor wind environment and thermal comfort at pedestrian level in housing blocks with different building layout patterns and trees arrangement. *Renewable Energy*, 73, 18–27. <http://dx.doi.org/10.1016/J.RENENE.2014.05.060>.
- Hong, B., Qin, H., & Lin, B. (2018). Prediction of wind environment and indoor/outdoor relationships for PM2.5 in different building–tree grouping patterns. *Atmosphere*, 9(2), 39. <http://dx.doi.org/10.3390/ATMOS9020039>, <https://www.mdpi.com/2073-4433/9/2/39/htm>.
- Hong, S. W., Zhao, L., & Zhu, H. (2018). CFD simulation of airflow inside tree canopies discharged from air-assisted sprayers. *Computers and Electronics in Agriculture*, 149, 121–132. <http://dx.doi.org/10.1016/J.COMPAG.2017.07.011>.
- Hsieh, C. M., & Huang, H. C. (2016). Mitigating urban heat islands: A method to identify potential wind corridor for cooling and ventilation. *Computers, Environment and Urban Systems*, 57, 130–143. <http://dx.doi.org/10.1016/J.COMPENVURBSYS.2016.02.005>.
- Jeanjean, A., Hinchliffe, G., McMullan, W., Monks, P., & Leigh, R. (2015). A CFD study on the effectiveness of trees to disperse road traffic emissions at a city scale.

- Atmospheric Environment*, 120, 1–14. <http://dx.doi.org/10.1016/j.atmosenv.2015.08.003>, URL <https://www.sciencedirect.com/science/article/pii/S135223101530248X>.
- Kang, G., Kim, J. J., & Choi, W. (2020). Computational fluid dynamics simulation of tree effects on pedestrian wind comfort in an urban area. *Sustainable Cities and Society*, 56, Article 102086. <http://dx.doi.org/10.1016/J.SCS.2020.102086>.
- Katul, G. G., Mahrt, L., Poggi, D., & Sanz, C. (2004). ONE- and TWO-equation models for canopy turbulence. *Boundary-Layer Meteorology*, 113(1), 81–109. <http://dx.doi.org/10.1023/B:BOUN.0000037333.48760.E5>, URL <https://link.springer-com.tudelft.idm.oclc.org/article/10.1023/B:BOUN.0000037333.48760.e5>.
- Kenjereš, S., & Ter Kuile, B. (2013). Modelling and simulations of turbulent flows in urban areas with vegetation. *Journal of Wind Engineering and Industrial Aerodynamics*, 123(PA), 43–55. <http://dx.doi.org/10.1016/J.JWEIA.2013.09.007>.
- Lalic, B., & Mihailovic, D. (2004). An empirical relation describing leaf-area density inside the forest for environmental modeling. *Journal of Applied Meteorology - J APPL METEOROL*, 43, 641–645. [http://dx.doi.org/10.1175/1520-0450\(2004\)043<0641:AERDLD>2.0.CO;2](http://dx.doi.org/10.1175/1520-0450(2004)043<0641:AERDLD>2.0.CO;2).
- Lauder, B., & Spalding, D. (1974). The numerical computation of turbulent flows. *Computer Methods in Applied Mechanics and Engineering*, 3(2), 269–289. [http://dx.doi.org/10.1016/0045-7825\(74\)90029-2](http://dx.doi.org/10.1016/0045-7825(74)90029-2), URL <https://www.sciencedirect.com/science/article/pii/0045782574900292>.
- Liang, X., Kankare, V., Hyyppä, J., Wang, Y., Kukko, A., Haggrén, H., Yu, X., Kaartinen, H., Jaakkola, A., Guan, F., Holopainen, M., & Vastaranta, M. (2016). Terrestrial laser scanning in forest inventories. *ISPRS Journal of Photogrammetry and Remote Sensing*, 115, 63–77. <http://dx.doi.org/10.1016/J.ISPRSJPRS.2016.01.006>.
- Liang, L., Xiaofeng, L., Borong, L., & Yingxin, Z. (2006). Improved k- ϵ two-equation turbulence model for canopy flow. *Atmospheric Environment*, 40(4), 762–770. <http://dx.doi.org/10.1016/J.ATMOSENV.2005.10.010>.
- Ma, H., Zhou, X., Tominaga, Y., & Gu, M. (2022). CFD simulation of flow fields and pollutant dispersion around a cubic building considering the effect of plume buoyancies. *Building and Environment*, 208, Article 108640. <http://dx.doi.org/10.1016/j.buildenv.2021.108640>, URL <https://www.sciencedirect.com/science/article/pii/S0360132321010313>.
- Maison, A., Flageul, C., Carissimo, B., Wang, Y., Tuzet, A., & Sartelet, K. (2022). Parameterizing the aerodynamic effect of trees in street canyons for the street network model MUNICH using the CFD model code_Saturne. *Atmospheric Chemistry and Physics*, 22(14), 9369–9388.
- Manickathan, L. (2019). Impact of vegetation on urban microclimate. (Doctoral Thesis), ETH Zurich, <http://dx.doi.org/10.3929/ETHZ-B-000379379>.
- Manickathan, L., Defraeye, T., Allegrini, J., Derome, D., & Carmeliet, J. (2018). Parametric study of the influence of environmental factors and tree properties on the transpirative cooling effect of trees. *Agricultural and Forest Meteorology*, 248, 259–274. <http://dx.doi.org/10.1016/J.AGRFORMET.2017.10.014>.
- Mohamed, M. A., & Wood, D. H. (2015). Computational study of the effect of trees on wind flow over a building. *Renewables: Wind, Water, and Solar*, 2(1), 1–8.
- Moradpour, M., Afshin, H., & Farhanieh, B. (2017). A numerical investigation of reactive air pollutant dispersion in urban street canyons with tree planting. *Atmospheric Pollution Research*, 8(2), 253–266. <http://dx.doi.org/10.1016/J.APR.2016.09.002>, URL https://www.researchgate.net/publication/308599202_A_numerical_investigation_of_reactive_air_pollutant_dispersion_in_urban_street_canyons_with_tree_planting.
- Ortega-Córdova, L. (2018). Urban vegetation modeling 3D levels of detail. (Master Thesis), Delft University of Technology, URL <https://repository.tudelft.nl/islandora/object/uuid:8b8967a8-0a0f-498f-9d37-71c6c3e532af?collection=education>.
- PDOK (2021). AHN3. URL <https://app.pdok.nl/ahn3-downloadpage/>.
- Peters, R., Dukai, B., Vitalis, S., van Liempt, J., & Stoter, J. (2022). Automated 3D reconstruction of LoD2 and LoD1 models for all 10 million buildings of the Netherlands. *Photogrammetric Engineering and Remote Sensing*, 88(3), 165–170. <http://dx.doi.org/10.14358/PERS.21-00032R2>, URL <https://www.ingentaconnect.com/content/asprs/pers/2022/00000088/00000003/art00011>.
- Ricci, A., Guasco, M., Caboni, F., Orlanno, M., Giachetta, A., & Repetto, M. P. (2022). Impact of surrounding environments and vegetation on wind comfort assessment of a new tower with vertical green park. *Building and Environment*, 207, <http://dx.doi.org/10.1016/j.buildenv.2021.108409>.
- Ricci, A., Kalkman, I., Blocken, B., Burlando, M., Freda, A., & Repetto, M. P. (2017). Local-scale forcing effects on wind flows in an urban environment: Impact of geometrical simplifications. *Journal of Wind Engineering and Industrial Aerodynamics*, 170, 238–255. <http://dx.doi.org/10.1016/j.jweia.2017.08.001>.
- Roache, P. J. (1994). Perspective: A method for uniform reporting of grid refinement studies. *Journal of Fluids Engineering*, 116(3), 405–413. <http://dx.doi.org/10.1115/1.2910291>, arXiv:https://asmedigitalcollection.asme.org/fluidsengineering/article-pdf/116/3/405/5531128/405_1.pdf.
- Salim, S. M., Cheah, S. C., & Chan, A. (2011). Numerical simulation of dispersion in urban street canyons with avenue-like tree plantings: Comparison between RANS and LES. *Building and Environment*, 46(9), 1735–1746. <http://dx.doi.org/10.1016/j.buildenv.2011.01.032>, URL <https://www.sciencedirect.com/science/article/pii/S0360132311000710>.
- Salmond, J. A., Tadaki, M., Vardoulakis, S., Arbutnot, K., Coutts, A., Demuzere, M., Dirks, K. N., Heaviside, C., Lim, S., MacIntyre, H., McInnes, R. N., & Wheeler, B. W. (2016). Health and climate related ecosystem services provided by street trees in the urban environment. *Environmental Health: A Global Access Science Source*, 15, <http://dx.doi.org/10.1186/S12940-016-0103-6>.
- Santiago, J. L., Buccolieri, R., Rivas, E., Calvete-Sogo, H., Sanchez, B., Martilli, A., Alonso, R., Elustondo, D., Santamaría, J. M., & Martin, F. (2019). CFD modelling of vegetation barrier effects on the reduction of traffic-related pollutant concentration in an avenue of Pamplona, Spain. *Sustainable Cities and Society*, 48, Article 101559. <http://dx.doi.org/10.1016/J.SCS.2019.101559>.
- Sanz, C. (2003). A note on k - ϵ modelling of vegetation canopy air-flows. *Boundary-Layer Meteorology*, 108(1), 191–197. <http://dx.doi.org/10.1023/A:1023066012766>, URL <https://link.springer-com.tudelft.idm.oclc.org/article/10.1023/A:1023066012766>.
- Sousa, J., & Gorié, C. (2019). Computational urban flow predictions with Bayesian inference: Validation with field data. *Building and Environment*, 154, 13–22. <http://dx.doi.org/10.1016/j.buildenv.2019.02.028>.
- Szkordilisz, F., & Zöld, A. (2016). Effect of vegetation on wind-comfort. *Applied Mechanics and Materials*, 824, 811–818. <http://dx.doi.org/10.4028/WWW.SCIENTIFIC.NET/AMM.824.811>, URL <https://www.scientific-net.tudelft.idm.oclc.org/AMM.824.811>.
- Vos, P. E., Maiheu, B., Vankerkom, J., & Janssen, S. (2013). Improving local air quality in cities: To tree or not to tree? *Environmental Pollution*, 183, 113–122. <http://dx.doi.org/10.1016/J.ENVPOL.2012.10.021>.
- Weller, H. G., Tabor, G., Jasak, H., & Fureby, C. (1998). A tensorial approach to computational continuum mechanics using object-oriented techniques. *Computers in Physics*, 12, <http://dx.doi.org/10.1063/1.168744>.
- Zheng, X., & Yang, J. (2021). CFD simulations of wind flow and pollutant dispersion in a street canyon with traffic flow: Comparison between RANS and LES. *Sustainable Cities and Society*, 75, Article 103307. <http://dx.doi.org/10.1016/j.scs.2021.103307>, URL <https://www.sciencedirect.com/science/article/pii/S2210670721005837>.